INFORMATION TO USERS

This manuscript has been reproduced from the microfilm master. UMI films the text directly from the original or copy submitted. Thus, some thesis and dissertation copies are in typewriter face, while others may be from any type of computer printer.

The quality of this reproduction is dependent upon the quality of the copy submitted. Broken or indistinct print, colored or poor quality illustrations and photographs, print bleedthrough, substandard margins, and improper alignment can adversely affect reproduction.

In the unlikely event that the author did not send UMI a complete manuscript and there are missing pages, these will be noted. Also, if unauthorized copyright material had to be removed, a note will indicate the deletion.

Oversize materials (e.g., maps, drawings, charts) are reproduced by sectioning the original, beginning at the upper left-hand corner and continuing from left to right in equal sections with small overlaps. Each original is also photographed in one exposure and is included in reduced form at the back of the book.

Photographs included in the original manuscript have been reproduced xerographically in this copy. Higher quality 6" x 9" black and white photographic prints are available for any photographs or illustrations appearing in this copy for an additional charge. Contact UMI directly to order.

UMI

A Bell & Howell Information Company
300 North Zeeb Road, Ann Arbor MI 48106-1346 USA
313/761-4700 800/521-0600

Evidence for Myosin in *Tetrahymena*

by

Jorge Garcés

A dissertation submitted to the Graduate Faculty in Biology
in partial fulfillment of the requirements for the degree of
Doctor of Philosophy, The City University of New York

1996

This manuscript has been read and accepted for the Graduate Faculty in Biology in satisfaction of the dissertation requirement for the degree of Doctor of Philosophy.

5/10/96
Date

Chairman of Examining Committee
Dr. Ray H. Gavin, Brooklyn College

5/21/96
Date

Executive Officer Dr. Richard L. Chappell

Dr. Jack R. Collier, Brooklyn College

Dr. Dan Eshel, Brooklyn College

Dr. Peter N. Lipke, Hunter College

Dr. Peter Satir
Albert Einstein College of Medicine

Supervising Committee

The City University of New York

Abstract

Evidence for Myosin in *Tetrahymena*

by

Jorge Garcés

Adviser: Professor R. H. Gavin

The objective of this study was to provide evidence for myosin in *Tetrahymena*. A combination of immunochemical, biochemical and PCR-based approaches have been employed to identify myosin-like proteins and myosin gene sequences.

Anti-myosin antibodies were affinity-purified from an antiserum raised against a *Tetrahymena* cytoskeletal protein fraction. The anti-myosin antibodies detected a 180 kD protein on western blots and immunoprecipitated the polypeptide from cytoskeletal protein fractions. The 180 kD protein exhibited an ATPase activity characteristic of myosins and was shown to bind skeletal muscle actin filaments in an ATP-dependent fashion. Immunofluorescence and immunogold electron microscopy were used to localize the p-180 to basal-body associated fibrillar structures and other cell constituents.

PCR-based screens for myosin in *Tetrahymena* have identified a sequence that shares a high degree of homology to other myosins. Alignment of the deduced amino acid sequence from approximately 2,000 bp of the *Tetrahymena* sequence with myosin consensus sequences revealed several shared conserved amino acid regions. Based on these amino acid alignments, we have concluded that the PCR-based screen has detected TETMYO-1,the first myosin gene in *Tetrahymena*.

Acknowledgements

Este libro es dedicado a mis queridos padres Amparo y Oscar Garcés quienes han sido mis mejores maestros y consejeros, sacrificando siempre sus propios sueños para que yo pudiera lograr los mios. Espero que Dios me los cuide y bendiga siempre. Madre, como te quiero...Padre, como te admiro...

To my wife, Marlene, whose love and support will always fill my life with purpose and meaning.

To my most altruistic friend, Ray, who always found himself on the giving end of things. I thank you and will miss you when I am gone.

Table of Contents

List of Tables

List of Figures

STRUCTURE OF MYOSIN

All myosins are complex multidomain proteins with the ability to generate unidirectional chemomechanical force. The architectural construct of the molecule includes three distinct domains (Rayment, et al. 1993a; Spudich, 1994; Mooseker and Cheney, 1995). A conserved 80 kD globular head region contains the N-terminus end of the protein and displays the ability to bind actin as well as ATP. A variable neck region associates with the light chain components (calmodulin or members of the EF-hand family of proteins) of the myosin complex. The regulatory neck domain of all myosins contains at least one light-chain binding motif called the IQ motif (Cheney and Mooseker, 1992). The IQ motif consists of a basic and hydrophobic 20-25 amino acid stretch that conforms to the consensus sequence: IQXXXRGXXXRXXY(W) (Xie et al., 1994). In conventional myosin, the essential and regulatory light chains have lost their ability to bind calcium specifically and two less-conserved repeats of the IQ motif correspond to their binding sites (Xie et al., 1994; Rayment et al., 1993a). Together, the head and neck regions constitute the motor domain of the molecule. In the presence of ATP, the motor domain is able to catalyze the hydrolysis of ATP and undergo the conformational adjustments that enable it to translocate along actin filaments. A C-term tail determines where the force is applied and accounts to a certain extent for the diversity of the different myosin isoforms. The tail regions of different myosins are structurally and chemically divergent and therefore functionally specialized. The tail domain localizes the motor protein within the cell by harnessing the molecule to an assortment of cellular substrates (reviewed by Titus, 1993; Mooseker and Cheney, 1995).

This variable region of the myosin molecule may also contain sequence motifs that are common to other proteins involved in a variety of signaling pathways (Bähler, 1996). Figure 1 below depicts the general structure of a myosin motor:

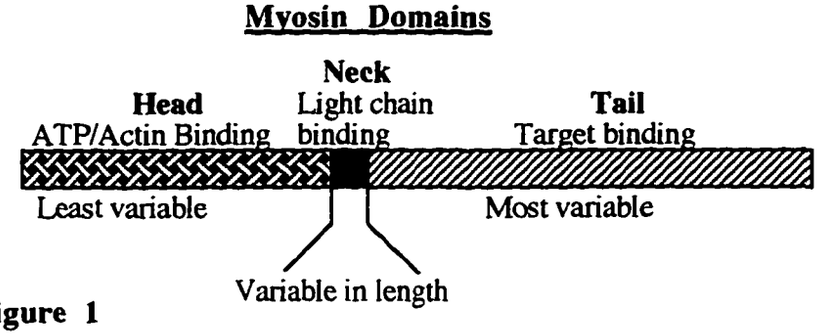

Figure 1

Structure of Sub-fragment 1

The structure of the myosin head domain had proved difficult to ascertain. The difficulty stemmed in part from the large size and intrinsic flexibility of the protein. Additionally, depending on the method of isolation, the molecule was prone to proteolytic digestion resulting in a large degree of heterogeneity. Eventually, the molecule was stabilized by reductively methylating all of its lysine residues (Rayment et al., 1993a). It could be argued that the chemical modification of myosin sub-fragment 1 could conceivably alter the structure in a profound manner. In an effort to add certainty to the structural data, Rayment and coworkers have reported that the kinetics of the modified motor remain unchanged and that the structure of lysozyme is not seriously altered by methylation (White and Rayment, 1993; Rypniewski et al., 1993). The structure of the regulatory domain of scallop myosin S1 was subsequently resolved and although the scallop myosin fragment was crystallized without the need for

methylation, its structure was virtually identical to the corresponding region of the methylated chicken S1 (Xie et al., 1994).

Any description of the S1 structure requires a definition of parts. Conventional myosin II is a double-headed, dimeric structure consisting of two identical heavy chains that are intertwined via the tail domain into an alpha-helical coiled-coil (reviewed by Titus, 1993). Each heavy chain comprises three major functional domains: a head, neck and tail from N- to C-terminus, respectively (reviewed by Wolenski, 1995). The globular head domain contains the actin and nucleotide-binding sites of the protein. The neck region is believed to act as the lever arm in the production of the powerstroke and contains the binding sites for the myosin light chains. The tail domain is involved in the dimerization of the heavy chains that interact to form the bipolar filaments which assemble into the superstructures known as thick filaments (Cheney and Mooseker, 1992). Myosin II has become the prototype (i.e. conventional myosin) for the study of all other actin-based motors because it has been the most widely investigated isoform and the first to be discovered. In fact, all other myosin isoforms are referred to as unconventional myosins.

The molecule is proteolytically cleaved into two parts following treatment with trypsin (Lowey et al., 1969; Margossian and Lowey, 1982). The larger portion consisting of the dimeric head, neck and part of the tail is called heavy meromyosin or HMM. The remaining piece of the tail is referred to as light meromyosin or LMM. Extensive treatment of the HMM fragment with trypsin or papain yields two pairs of fragments, S1 and S2 (see figure 2). S1, devoid of the tail and no longer able to dimerize, consists of the head and neck regions of the myosin molecule. S2 consists of the tail fragment between the neck and the

cleavage site that separates HMM and LMM. It has been speculated that the site of cleavage corresponds to the hinge region of the molecule.

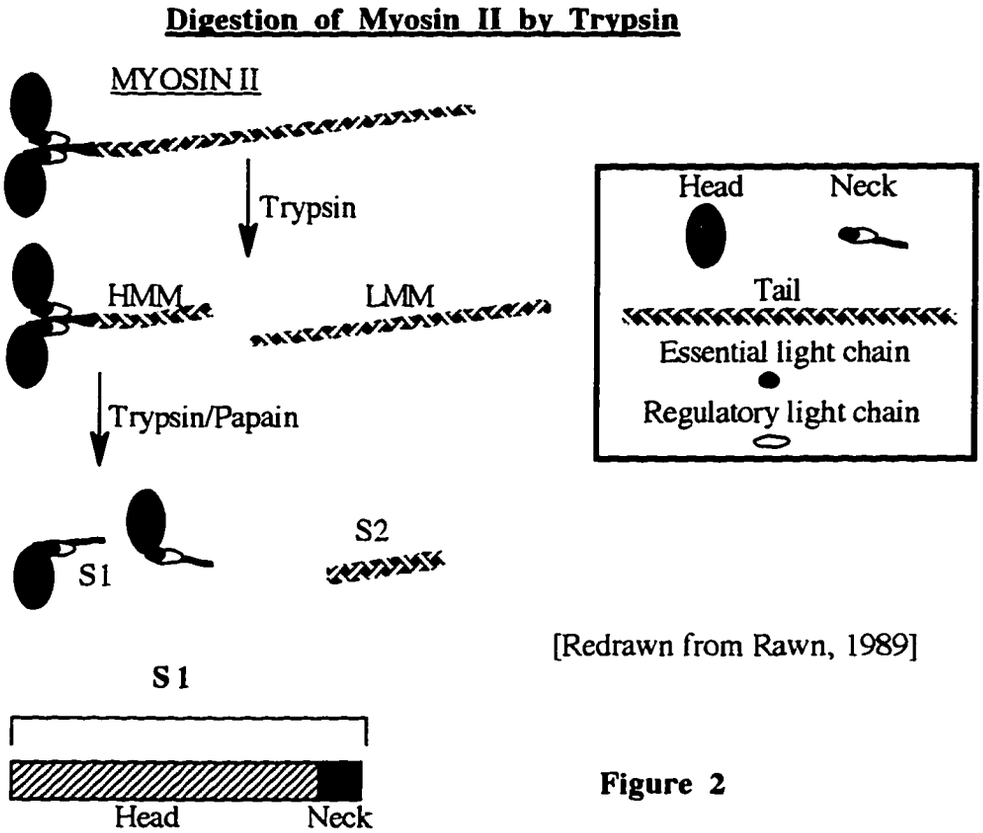

[Redrawn from Rawn, 1989]

Figure 2

S1 can be further digested by trypsin into three fragments of 25 kD, 50 kD, and 20 kD from N- to C- terminus, respectively (Mornet et al., 1979). It had been postulated that these fragments corresponded to structural domains, but instead, the pattern of digestion reflects the location of cleavage sites within disordered loops that are susceptible to digestion (Rayment et al., 1993a). The structural data reveals a deep cleft that extends from the nucleotide-binding pocket to the actin-binding interface and splits the 50 kD fragment into two parts that are

referred to as the upper and lower 50 kD fragments. The upper 50 kD fragment is contiguous with the C-terminal part of the N-terminal most 25 kD fragment. It contains a seven-stranded β-sheet flanked by α-helices or loops and encompasses the nucleotide-binding site. The nucleotide binds to a broad depression on one side of the molecule which leaves it uncharacteristically exposed to the solvent (Rayment et al., 1993a). In contrast, actin and most other proteins accommodate the nucleotide within a deep cleft (Kabsch et al., 1990). The lower 50 kD fragment consists of long α-helices, one of which is part of the 20 kD fragment. The actin-binding site is composed from residues found in both the upper and lower 50 kD fragments as well as those that constitute the first α-helix of the 20 kD fragment located at the 50/20 kD junction (see figure 3). In order to couple the energy available from the hydrolysis of ATP to the sliding of actin, the actin - and nucleotide-binding sites must relate information to each other. The problem is that the two sites lie on opposite sides of the molecule at a distance of approximately 4 nm apart (Spudich, 1994). Recent focus has centered around the issue of inter-communication between domains and the ability to convert protein conformational shifts into unidirectional movements (Shriver, 1984; Schulz, 1991).

A second striking feature of the structure is the long, 8.5 nm α-helix that forms the neck region (Rayment et. al 1993a; Xie et al., 1994). The two light chains wrap around the helix in a somewhat protective fashion as illustrated in figure 3. Interestingly, they share sequence homology with the calmodulin family of proteins which bind their respective ligands in a similar manner (Kretsinger and Kawasaki, 1994). There are two disordered surface loops that deserve mentioning, but because of their intrinsic flexibility remained unresolved as part

of the structure. The loops are poorly conserved in both length and sequence, but their importance has been demonstrated (Sweeney, 1994; reviewed by Ruppel and Spudich, 1995). Loop 1 is found in the vicinity of the nucleotide-binding pocket and loop 2 is at the actin-binding site.

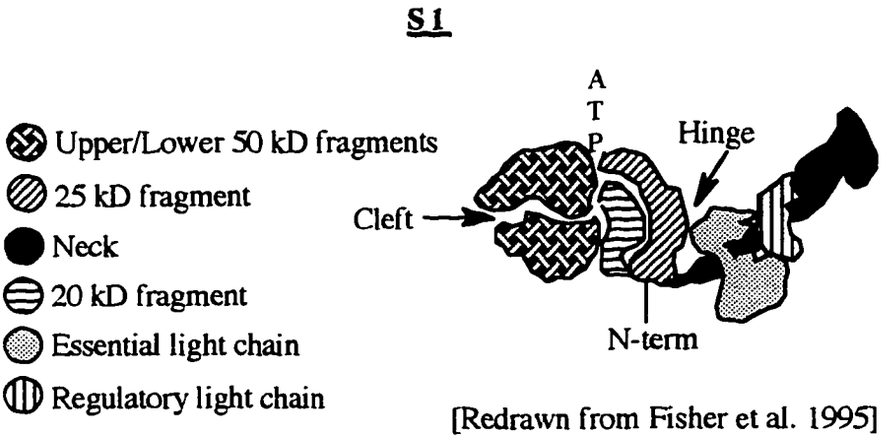

Figure 3

Variability in the Structure of Myosin Isoforms

Conventional myosin or myosin II was first identified in frog muscle extracts one hundred and thirty years ago by Kuehne (1864). As a prominent component of muscle, myosin has been extensively studied due to its fundamental role in muscle contraction. The distinctive biochemical properties of muscle myosin were employed to identify the protein in non-muscle cells and assay its role in cell motility. The biochemical criteria for myosin included an actin-activated ATPase activity, ATP-sensitive binding to actin and the ability to translocate actin filaments in a nucleotide-dependent fashion. Aside from its significance in force generation during muscle contraction, the actin-based

molecular motor turned out to be a critical component in a wide array of nonmuscle movements (reviewed by Korn and Hammer, 1988; Spudich, 1989; Kiehart, 1990). Biochemical analysis of cytoplasmic cell extracts lead not only to the discovery of muscle myosin in non-muscle cells (Warrick and Spudich, 1987; Korn and Hammer, 1988), but the isolation of the first unconventional myosin in *Acanthamoeba* (Pollard and Korn, 1973). The initial description of a short-tailed, non-filamentous myosin (myosin I) met with skepticism, especially because conventional myosin (myosin II) could be easily degraded by endogenous proteases during isolation procedures. One of the degradation products, S1, was the globular, non-filamentous, enzymatically active myosin II head fragment similar in structure to myosin I (Korn and Hammer, 1990). The rediscovery of myosin I in chicken intestinal brush border as an ATP-soluble, 110 kDa protein that cross-linked and tethered the microvillar core bundle to the plasma membrane reinforced the existence of unconventional myosin isoforms (Pollard et al., 1991; Mooseker et al., 1991). Subsequently, it became evident that myosin I was an essential element in a number of actin-based activities (Korn and Hammer, 1990; Pollard et. al, 1991) that were independent of myosin II function. Aside from the apparent functional divergence, these isoforms also differed structurally. Conventional myosin dimerized and assembled into bipolar filaments via the tail domain, but unconventional myosin was monomeric and its tail domain lacked the extensive α-helical coiled-coil structure of conventional myosin. Due to the seemingly clear dichotomy in structure, the myosins were categorized into two groups: the conventional two headed, dimeric myosins (myosin II) and their non -filamentous monomeric counterparts, the unconventional myosins (myosin I)

(reviewed by Warrick and Spudich, 1987; Korn and Hammer, 1988; Pollard et al., 1991). But the structural diversity of newly characterized myosins complicated the issue of classification (reviewed by Cheney and Mooseker, 1992; Titus, 1993). One example was the product of the *Drosophila ninaC* gene which encoded a novel actin-based motor that was astoundingly different from either of the two known myosin classes in that it contained an N-terminal extension consisting of a protein kinase domain (Montell and Rubin, 1988). Clearly this myosin would constitute a different classification. Another class of unconventional myosins was exemplified by *Dilute*, p190, and MYO2 (Mercer et al., 1991; Espreafico et al., 1992; Johnston et al., 1991, respectively). Although, these myosins were compatible to myosin II in that they could potentially dimerize, unlike myosin II these myosins were unable to form filaments. The explosive rate at which new myosin isoforms were being discovered made it clear that the simple division of the actin-based motors into two classes was inadequate. Recently, investigators have grouped the different isoforms based on phylogenetic sequence comparisons of the head domains, and the classification scheme reflects differences in non-conserved sequences (neck and tail regions) quite accurately (Cheney et al., 1993a; Goodson and Spudich, 1993; Mooseker and Cheney, 1995). These molecular motors clearly emerged from a large, complex, widely distributed and evolutionary ancient superfamily of myosin genes (Mooseker and Cheney, 1995). It is generally believed that most cells, both plant and animal, have multiple forms of myosin and that each form within the multitude may be distinctively adapted (although functional redundancy is evident) for a given actin-based movement (Titus, et al., 1994; Bement et al., 1994; Kinkema, et al., 1994). The literature on

myosin is quite extensive and what appeared to be eight evolutionarily distinct classes of unconventional myosins (Cheney et al., 1993a) is now at least eleven (Mooseker and Cheney, 1995). Myosins are involved in virtually all facets of cell regulation including cytokinesis, karyokinesis, cell migration, capping of surface receptors, changes in cell shape, amoeboid movement, intracellular transport of membrane precursors, vesicle trafficking, contractile vacuole function and have been implicated in signal transduction pathways (Pollard et al., 1991; Johnston, et al., 1991; Fukui et al.1989; Doberstein et al., 1993; Fath and Burgess, 1994; Langford, 1995; Bähler, 1996). There is a torrent of information on the sequence, structure and biophysical properties of the many myosins. Their continued localization at the resolution of immunogold electron microscopy, genetic manipulation, structural classification and functional characterization will undoubtedly expand our understanding of the specific biological activities involving myosins (reviewed by Titus, 1993; Spudich, 1994; Mooseker and Cheney, 1995).

Some myosin classes contain multiple members while others are represented by a single member. The Myosin-I class is the largest and most diverse class of unconventional myosins. It has been divided into four distinct sub-classes (Hammer, 1994; Mooseker and Cheney, 1995). Most of the type-1 myosins have a relatively short head region and a neck region consisting of 1-3 IQ motifs. The tail regions contain different tail homology domains (TH1, TH2, TH3). The TH1 domain is the most common and it is usually located immediately C-terminal to the neck domain. It is rich in basic residues and effects binding of myosin to acidic phospholipids. The TH2 domain is an ATP-insensitive actin binding site that is also referred to as the GPA/GPQ domain

because it is rich in glycine, proline and either alanine of glutamine. Some myosins-I contain a TH3 domain homologous to SH3 domains in signal transduction factors known to bind proline rich motifs. Myosins-I are involved in various cellular functions ranging from cell movement and organelle transport (Pollard et al., 1991; Doberstein et al., 1993; Fath and Burgess, 1993) to the modulation of ion channels in hair cells (Assad and Corey, 1992). The functional aspects of these enzymes are not yet clearly defined and our discussions are often limited to sequence homology and the predicted structure of the proteins. The function and structure of myosin II have been extensively studied and are discussed in other sections.

Myosins-III are the most phylogenetically divergent myosins. The only members of the class III myosins are the two ninaC proteins found exclusively in the photoreceptor cells of *Drosophila melanogaster* where they are involved in phototransduction (Montell and Rubin, 1988). The *ninaC* (neither inactivation nor after-potential C) gene codes for two proteins, p132 and p174, derived from alternative RNA splicing occuring within sequences coding for the neck domain. Both of these myosins contain a serine/threonine kinase domain as an N-terminal extension of the head region. Another distinctive feature is that these myosins lack either a phosphorylatable or acidic residue at the TEDS rule site (Bement and Mooseker, 1995). The proteins are differentially localized. p174 is localized in the microvillar rhabdomeres and p132 is found in the cell body (Porter, et al., 1992). Mutational analysis of ninaC p174 revealed that it not only serves multiple roles in phototransduction and rhabdomere maintenance (Porter and Montell, 1993), but may also function in the proper localization of calmodulin in the photoreceptor cell (Porter et al., 1993). A p174 deletion

construct lacking the two IQ motifs in the neck domain exhibits abnormal calmodulin localization. Recently, it was shown that both calmodulin-binding sites are required *in vivo* for proper termination of phototransduction (Porter et al., 1995).

The sole member of the class IV myosins is the 177 kD high-molecular weight unconventional myosin of *Acanthamoeba* that was originally described as a myosin-I (Horowitz and Hammer, 1990). This protein has a 90-kDa head domain, a neck domain with a single IQ motif, and a novel 87-kDa tail domain. The lack of predicted coiled-coil structure in the tail suggests that myosin-IV is monomeric. Although the tail portion lacks the TH1 and TH2 domains characteristic of myosins-I, it contains a 50-residue SH3 domain near the C-terminus.

Next to myosins-I and II, the class V myosins are the most abundantly expressed and members have been identified in vertebrates and yeast (Mooseker and Cheney, 1995). Full length cDNA sequences have been obtained for the yeast *MYO2* and *MYO4* genes, mouse *dilute* gene, and the chicken brain myosin-V gene (Johnston et al., 1992; Haarer et al., 1994; Mercer et al., 1991; sanders et al., 1992; Espreafico et al., 1992). All four sequences code for myosins-V with homologous head domains. The neck domain of all four proteins contains six IQ motifs. The protein has been shown to dimerize and the tail end of the molecule terminates in a globular structure (Cheney et al., 1993b). There is strong evidence that this class of motors is involved in cytoplasmic vesicle motility. Chicken brain myosin-V is associated with vesicles in the golgi area of cultured neurons and has been identified as a component of the synaptic membrane (see review by Langford, 1995). Myosin

-V like all other known myosins is a plus-ended motor (Cheney et al., 1993b). Mutants in mouse and yeast have provided some clues into the possible functions of myosins-V. Myosin-V, encoded by the mouse *dilute* locus, has been shown to be involved in the formation or maintenance of melanocyte dendrites (Silvers, 1979). Homozygotes for the mouse *dilute* gene experience a dilution or lightening of their coat color due to a defect in the transport of the pigment-containing organelles called melanosomes from their site of synthesis to the keratinocytes of a growing hair. A similar disease known as Griscelli syndrome in humans is associated with pigmentary dilution (Griscelli, 1978). The yeast MYO2 protein is a myosin-V identified in a screen for temperature-sensitive cell division cycle mutants (Johnston et al., 1991). At the restrictive temperature, the *myo2* mutants fail to initiate bud formation and the large cells accumulate a great number of vesicles. Surprisingly, the mutant phenotype can be suppressed by overexpression of Smy1p, a kinesin-related protein (Lillie and Brown, 1992). The MYO2 protein binds calmodulin and co-localizes with Smy1p to regions of active cell growth and in actin spots (Brockerhoff et al., 1994; Lillie and Brown, 1994). Unfortunately, MYO4 studies have not been as informative and *myo4* gene deletions yield no aberrant phenotype. Myosins-V share a tail sequence motif in common with the gene products of human AF-6, a fusion partner of the ALL-1 gene involved in acute myeloid leukemias (Prasad et al., 1993) and *Drosophila* canoe protein involved in adhesive cell-cell interactions that act in a variety of developmental processes (Ponting, 1995; Miyamoto et al., 1995).

Drosophila 95F and Porcine myosin-VI are the two most prominent class VI myosins (Kellerman and Miller, 1992; Hasson and Mooseker, 1994). A PCR-

based approach has been used to uncover additional members of this class in humans and bullfrog (Bement et al., 1994; Solc et al., 1994). These myosins have a head-neck junction that differs from all other known myosins. The neck contains a single IQ motif. The tail region contains a coil-coiled domain and a globular domain that is more homologous among myosins-VI than the head region. Antibodies against the tail portion of pig myosin-VI have been used to identify immunogens in a wide range of vertebrate species including rat, mouse, human, chicken and *Xenopus*. Myosin-VI is localized to the proximal tubule in kidney where it is associated with the submicrovillar domain of the brush border (Hasson and Mooseker, 1994). The 95F myosin from *Drosophila* is required for the proper organization and division of nuclei in the syncytial blastoderm. Antibody inhibition assays have shown that the protein associates with granules of unknown composition and mediates their movement within the syncytial cytoplasm (Mermall et al., 1994; Mermall and Miller, 1995).

The first member of the class-VII myosins to be identified was myosin 35BC in *Drosophila* (Chen et al., 1991). A phylogenetic analysis of the partial head sequence for this myosin defines it as a new class of myosin (Mooseker and Cheney, 1995). Partial sequence information corresponding to myosins-VII have been obtained from pig and bullfrog (Bement et al., 1994; Solc et al., 1994). The neck domain contains five IQ motifs followed by a segment with predicted coiled-coil structure. Recently, studies on deafness in mice and humans have provided exciting insights into the function of class-VII myosins (Gibson et al., 1995; Wei et al., 1995). It appears that these motors are involved in auditory transduction. The mouse *shaker-1* deafness gene and its human orthologue, Usher syndrome 1B gene, encode murine and human

myosin VIIA. *Shaker-1* mice suffer from hearing loss and vestibular dysfunction due to the degeneration of the inner ear sensory epithelium (Steel and Brown, 1994). Usher syndrome 1B is associated with hearing impairment and blindness due to retinitis pigmentosa. The full cDNA of the Usher syndrome 1B gene is approximately 7 kb in size (Unpublished: accession no. U39226, GB; Weil et al., 1995). Northern and western blot analysis in other species indicates a transcript of >9 kb and a 240 kDa protein (Hasson et al., 1995). Myosin VIIA expression in the cochlea is restricted to the inner and outer hair cells of the sensory epithelium. It localizes specifically to the cell body and apical stereocilia of these cells. In the retina, myosin VIIA is exclusively found in pigmented epithelial cells (Hasson et al., 1995). The examination of other myosins-VII, specially *Drosophila* 35BC should provide more exciting clues on the function of these motors and their co-factors.

Arabidopsis thaliana myosins 1 and 2, ATM1 and ATM2, are the class-VIII plant myosins (Knight and Kendrick-Jones, 1993; Kinkema et al., 1994). There are N-terminal amino acid extensions in the head region of these myosins. ATM1 contains four IQ motifs and ATM2 contains three. These myosins may potentially form dimers via their highly homologous tail domains. Transcripts of ATM1 are found in leaf and root tissue. ATM2 is prevalent in flower and root tissues. Both myosins contain an aspartic acid at the TEDS rule phosphorylation site (Bement and Moosker, 1995).

The only myosin with a tail domain interacting signal transduction partner is myr 5, a class-IX myosin identified in rat (Reinhard et al., 1995). Partial cDNA's encoding class-IX myosins have been identified in pig and human species (Bement et al., 1994). There are large N-terminal extensions in these

myosins. There is also a large insertion at one of the loops (loop 2) known to interact with actin in myosin II molecules that may alter the mechanochemical properties of myosins-IX (Mooseker and Cheney, 1995). The neck domains of myosins-IX contain four IQ motifs. The most remarkable feature of these myosins is the composition of the tail region which is rich in proline but also contains a cysteine-rich domain that is similar in structure to the zinc and phospholipid binding motif of protein kinase C. A more intriguing feature is a region C-terminal to the zinc-binding domain, that is homologous to the GTPase-activating protein (GAP) known to stimulate the hydrolysis of GTP by the rho subfamily of G proteins (Reinhard et al., 1995). These small G proteins induce the reorganization of the actin cytoskeleton when found in their active GTP-bound conformation (Nobes and Hall, 1995). The structural layout of chimaerin, a GAP for the Rac members of the Rho subfamily, is similar to that of the tail region of myosins-IX in that a zinc-binding motif precedes a GAP domain (Hall, 1994). The myr 5 GAP domain has been shown to activate the GTPase of Rho (Reinhard et al., 1995). Myosins-IX appear to be monomeric. Human myosin-IXb is found in a large number of tissues, but the 8 kb transcript is expressed at high levels in leukocytes. The exact mechanism, pathway and time of action of myosins-IX are yet to be elucidated.

Another exotic group of myosins that emphasize the multifarious complexity of isoform structure and function are the myosins-X. Solc et al. (1994) have characterized both bullfrog and bovine myosin-X sequences. The neck region of bovine myosin-X contains three putative calmodulin binding sites. The tail domain has predicted coiled-coil structure and contains three PH (pleckstrin homology) domains (Mooseker and Cheney, 1995). PH domains are present in

many signal transduction proteins, but the function and target sites (particularly in myosins-X) of these domains are not thoroughly defined (Gibson et al., 1994). In order to assay the function of these myosins, the actual protein components (myosins and their signaling partners) must be isolated and biochemically analysed. Alternatively, new members of the class-X myosins must be identified in organisms amenable to genetic manipulation.

Several plant myosins contribute to form an eleventh class of actin-based motors. *Arabidopsis* MYA1 and MYA2 (Kinkema and Schiefelbein, 1994; Kinkema et al., 1994) as well as four other partial sequences in this organism code for myosins-XI. Recently, it was determined that the sequence of the *Dictyostelium* MYO J gene codes for a myosin that falls into this classification (Hammer and Jung, 1995). The high degree of similarity between these and class-V myosins makes the class-XI classification questionable. Hammer and Jung (1995) argue that although the class-V and class-XI myosins share some features in common, the 434-residue globular tail portion of myo J is different than that of yeast and vertebrate myosins-V. Phylogenetic analysis of the head regions of myo J and class-V myosins fails to group these myosins into one class. The class-XI myosins are dimeric and contain six IQ motifs. These motors have a glutamic acid residue at the TEDS rule site (Bement and Mooseker, 1995). Both MYA1 and MYA2 are differentially expressed in various plant tissues. Northern Blot analysis of myo J expression suggests that it may function primarily in vegetative *Dictyostelium* cells.

The next critical step towards understanding how unconventional myosins work will require the resolution of their crystal structures. All conventional myosins contain two sequential repeats of approximately 25 amino acids that

form an α-helix in the neck region of the motor molecule and serve as the light-chain binding sites. The swinging neck-lever model proposed by Rayment et al. (1993) suggests that the mechanical powerstroke is generated from conformational changes occurring in the globular head region of myosin and amplified by the neck region serving as a lever arm. In smooth muscle myosin II, weakening of the lever arm by removal of one or both light chains caused a 50-90% reduction in velocity *in vitro* (Lowey et al., 1993). Removal of the regulatory light chain binding site from *Dictyostelium* myosin II resulted in a truncated lever arm (50% shorter) and a 50% reduction in the rate of velocity (Uyeda and Spudich, 1993). Similarly, removal of both the regulatory and essential light chain binding sites resulted in an extremely truncated myosin neck with a 90% reduction in velocity (Itakura et al., 1993). These results support the model which predicts that a shorter lever arm would generate a smaller powerstroke following ATP hydrolysis. Conversely, a longer lever arm would result in a larger powerstroke. The unconventional myosin isoforms can contain anywhere from one to six light chain-binding sequences along the neck region. Therefore, the length of the lever arm varies between isoforms. Logically, it follows that there must be some degree of variability in the manner in which unconventional myosins operate. Despite the high degree of amino acid sequence conservation in the head region of different myosins, there is sufficient divergence between myosins to allow their arrangement into different classes and alter their enzymatic behavior. Aside from obvious structural differences in the neck and tail regions of conventional and unconventional myosins, it has been hypothesized that functional differences among myosin isoforms is derived from poorly conserved sequences in the head. Two highly

noticeable heterogeneous regions are the flexible loops 1 and 2 in the myosin motor domain. As previously mentioned, although these loops are poorly conserved in both length and sequence, they are located at critical sites. Loop 1 is adjacent to the ATP-binding site and loop 2 is located at the 50-20 kD junction known to be involved in actin-binding (Rayment et al., 1993; Spudich, 1995). To test this hypothesis, chimeric proteins consisting of a *Dictyostelium* myosin backbone and the *Dictyostelium* loop 2 replaced with that from skeletal muscle myosin, alpha- or beta-cardiac myosin, and chicken smooth muscle myosin (Uyeda et al., 1994) were constructed. The skeletal muscle myosin-*Dictyostelium* chimaera was 5-6 times more active than the native *Dictyostelium* motor protein as measured by the Vmax of its actin-activated ATPase activity. This chimeric myosin behaved more like skeletal muscle myosin from which the loop 2 sequence for the chimaera was derived. The smooth muscle-*Dictyostelium* chimaera exhibited an ATPase activity similar to that of smooth muscle and twofold less than that of native *Dictyostelium* myosin. The activity of alpha- and beta- cardiac myosin-*Dictyostelium* chimaeras was intermediate between the other two. It is believed that loop 2 may regulate the transition from a weak to strong binding state during the actomyosin interaction (Spudich, 1995). Variability in the amino acid sequence of loop 2 seems to alter this transition. Although comparable studies using loop 1 chimaeras have not been done, it is likely that this loop is also involved in some critical step of the ATPase cycle, such as the rate of ADP release following the powerstroke. It will be interesting to see data on the substitution of these loops using chimeric proteins derived from unconventional myosins.

HOW DOES MYOSIN WORK?

The Cross-Bridge Theory

In the sarcomere, the basic functional unit of muscle, myosin forms bipolar filaments that interdigitate with actin filaments to form cross-bridges (Huxley, 1957; Huxley and Simmons, 1971). Although it has been established that the shortening of muscle involves the sliding of these filaments relative to one another, the exact mechanism by which myosin converts the free energy derived from the hydrolysis of ATP into movement is still unclear. The cross-bridge model (Huxley, 1969; 1974) predicts that the sliding motion is powered by myosin cross-bridges that protrude from the myosin thick filament onto the thin actin filaments and act as oars to push the actin filaments as ATP is hydrolyzed. The model can easily be made to incorporate the actin-activated myosin ATPase cycle (Lymn and Taylor, 1971). The diagram in figure 4 below illustrates the principle steps in the interaction between myosin and its two substrates:

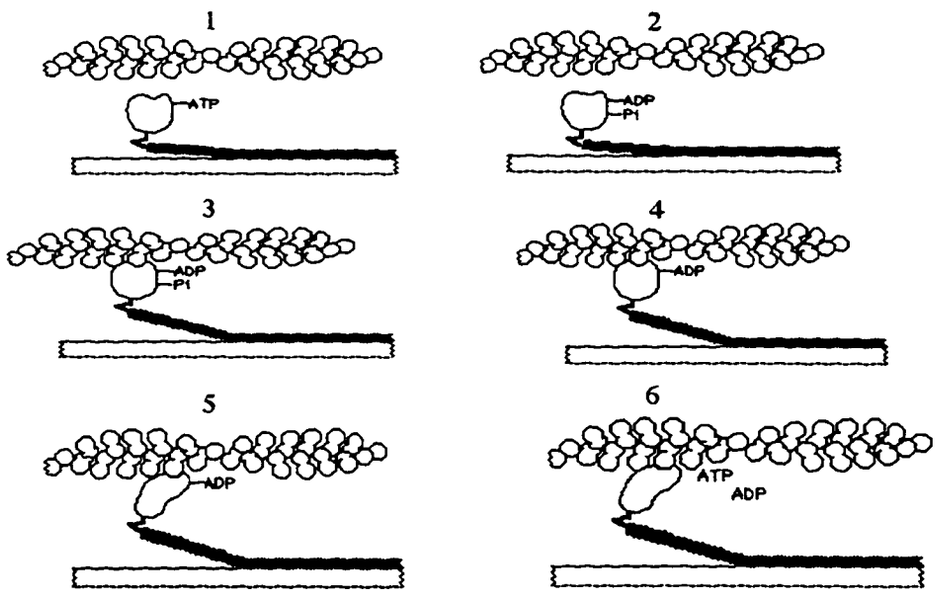

Figure 4 [Spudich, 1994]

There are several key elements to the model illustrated above (Adelstein and Eisenberg, 1980; Cooke, 1986; Goldman, 1987; Geeves, 1991). First, the cross -bridges are formed by the head domains of the myosin molecule. Second, the dissociation of the actomyosin complex is coupled to the binding of ATP (Taylor, 1991). Third, the force production step, referred to as the powerstroke is closely associated with the release of phosphate following ATP hydrolysis (Lymn and Taylor, 1971). In the absence of ATP, actin and myosin are tightly bound in a rigor complex. The binding of ATP to the globular head region of the myosin molecule induces the release of actin from myosin. Shortly after the exchange of ligands by myosin, the bound ATP is rapidly hydrolyzed to yield ADP and Pi. These remain associated with the motor and at this point the affinity of myosin for actin is low. A series of conformational shifts in alternate regions of the myosin molecule are coupled to the release of phosphate (Lymn and Taylor, 1971). These isomerizations allow the motor to bind actin with a higher affinity, but in a strained orientation. The release of the "cocked" myosin from the strained conformation marks the transition from a pre-stroke to a post-stroke state and results in force production (Spudich, 1994). Since the tail portion of the myosin is anchored to a bipolar filament, the stroke leads to the movement of the myosin head region and the sliding of the firmly held actin filament relative to the myosin thick filament. The massive conformational changes that are associated with the powerstroke trigger the release of ADP from myosin (Siemankowski and White, 1984). The cycle continues with the binding of ATP to the catalytic site of myosin.

Technology Provides A Closer Look

The complexity of the conformational changes that myosin and actin

experience during the actomyosin interaction had not been fully appreciated until recently (See reviews by Spudich, 1994; Vale, 1994; Cooke, 1995; Holmes, 1995). Two innovative approaches have extended our understanding of the molecular mechanism involved in actomyosin-based movement. First, the X-ray crystal structure of both actin and myosin sub-fragment 1 (S1) have been resolved in the first half of this decade (Kabsch et al., 1990; Rayment et al., 1993a). These structures were fit into the quarternary complex of the S1 decorated actin filament using electron micrographs and fiber diffraction data (Rayment et al., 1993b; Schroder et al., 1993). These structural data have led to a novel hypothesis concerning the nature of the conformational changes involved in the interaction between the two molecules as well as the molecular mechanics implicated in the generation of force (Rayment and Holden, 1994). Second, advances in the field of microscopic technology and in vitro motility assays have provided direct measurements of force and displacement from a single myosin molecule (Ishijima et al., 1994; Finer et al., 1994).

Actin Structure

It had proved quite problematic to elucidate the structure of the G-actin monomer due to the tendency for polymerization. In order to overcome this predicament, the structure had to be resolved from crystals of actin in complex with DNase I, a protein known to inhibit actin polymerization (Kabsch et al., 1990). Surprisingly, the structure of G-actin resembles that of two functionally unrelated proteins, hsp-70 and hexokinase B (Bork et al., 1992). In the conventional frontal view of actin, the monomer resembles a thick slice of a cube with a side length of 5-6 nm and a thickness of 3.5 nm. Actin and its structural counterparts are divided by a deep cleft that serves as the site of nucleotide and

cation binding. The cleft divides the molecule vertically into two domains of roughly equal size. The two domains have been further divided into a total of four subdomains as illustrated in figure 5 below:

Structure of Actin

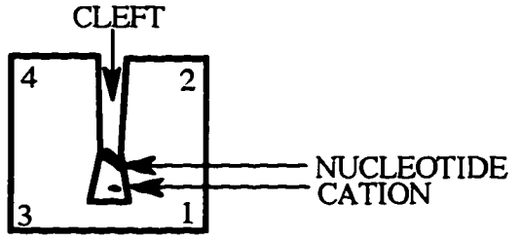

Figure 5

Subdomains 1 and 3 denote a hinge region of the molecule with the potential for relative movement of the domains. These two subdomains are connected by only two strands of the polypeptide chain and ATP provides a major bridge between them. The nucleotide species (ATP or ADP) may determine the relative orientation of the subdomains (Sheterline and Sparrow, 1994). The N- and C -termini of the polypeptide reside in subdomain 1. In this representation, the subdomains 1 and 3 would face the plus end of the F-actin polymer. In the F -actin polymer, two strands are helically intertwined such that subdomains 1 and 2 are located on the outside of the filament while subdomains 3 and 4 of each strand hold together the center of the polymer (Holmes et al., 1990).

DNase I binds to actin at subdomains 2 and 4 of the monomer (Kabsch et al., 1990). It was difficult to judge the validity of the actin structure in complex with DNase I, but structural data available from actin/gelsolin segment 1 crystals and actin/profilin crystals show only a small degree of variability in the structure of

actin (McLaughline et al., 1993; Schutt et al., 1993). Both gelsolin and profilin bind to the opposite end of the monomer at subdomains 1 and 3, suggesting that the association of actin-binding proteins with actin does not significantly alter its structure.

Structure of the Rigor Complex

An atomic model of the actomyosin rigor complex (the tight bond formed between actin and myosin in the absence of ATP) was determined by overlapping the structure of myosin and F-actin using three-dimensional reconstructions assembled from low-resolution electron micrographs of the complex (Rayment et al., 1993b; Schroder et al., 1993). The myosin fits quite nicely into the actin filament structure, but steric collisions in the docking were avoided only when the cleft was closed. A new model that explains the conformational changes involved in the production of the powerstroke was formulated from this structure (Rayment et al., 1993b). The actomyosin interaction involves components from both the upper and lower 50 kD fragments that protrude from each side of the cleft as well as those found along the 50/20 kD junction. Myosin and actin may potentially interact in three different ways. The initial weak contact probably involves an ionic interaction between the acidic residues at the N-terminus of actin and the basic lysines of loop 2 at the 50/20 kD junction of S1. This interaction could occur at a long range and in a wide variety of orientations. The main contact presumably involves the interaction between hydrophobic residues on helix-loop-helix motifs found through out the upper and lower 50 kD fragments of S1 and those on the strands linking subdomains 1 and 3 of actin. Subdomain 1 also participates in the strong interaction along with subdomain 2 on the next actin monomer along the filament. Finally, an ordered loop at the TEDS rule site for

phosphorylation interacts with actin (Bement and Mooseker, 1995). Specific point mutations within this loop have been linked to an illness known as familial hypertrophic cardiomyopathy and have been shown to alter the ATPase activity of the enzyme (Geisterfer-Lowrance et al., 1990; Sweeney et al., 1994). In summary, myosin binds across two actin molecules deeply into the filament (Amos et al., 1982; Andreev and Borejdo, 1991).

NEW PERSPECTIVES

The Swinging Neck-Lever Model

As stated earlier, in the absence of ATP, actin and myosin are tightly bound in a rigor complex. The addition of ATP is believed to open the cleft that splits the 50 kD fragment of S1. Opening the cleft disrupts the tight stereospecific actin-myosin interaction. This is predicted to occur through a series of steps that would prevent any reversal in the powerstroke (Rayment et al., 1993b). The ATP-bound myosin returns to its pre-stroke conformation and the head region is free to rotate as it forms transient interactions with actin that are weak, ionic, and non-stereospecific (Geeves, 1992). The hydrolysis of ATP leaves myosin bound to ADP and Pi in a final pre-stroke conformation. The molecule binds actin through a multi-step process to assure that the motor be positioned in the proper orientation relative to the actin filament. In order to generate unidirectional movement, myosin and actin must be properly oriented relative to one another before forming the tight bond that fastens the two molecules together during the powerstroke. The head region of myosin remains firmly bound to actin in the same relative orientation as the powerstroke is produced by a rotation of the neck

region. It had been proposed that the conformational changes associated with the powerstroke were produced by opening of the nucleotide pocket (Rayment and Holden, 1994), but recent studies using spectroscopic probes attached to the catalytic domain and structural data on nucleotide-bound S1 suggest that the nucleotide-binding pocket is relatively ordered during the powerstroke (Crowder and Cooke, 1987; Franks-Skiba and Cooke, 1995; Fisher et al., 1995). According to the latest model (Fisher et al. 1995), subsequent to the formation of the tight bond between actin and myosin, the lower 50 kD fragment moves relative to the upper 50 kD fragment. This movement results in both the release of phosphate and closure of the cleft that divides the upper and lower 50 kD fragments. The phosphate group leaves myosin through a site different from that in which it entered leaving ADP bound (Yount et al., 1995). The movements occuring at the 50 kD region are initially transmitted to the 20 kD fragment and eventually to the light chain-binding region of the the neck. In order to transform conformational changes into rotational movement, there must be a hinge within the molecule. The C-terminus of the essential light chain and the 25 kD fragment of the head are likely to interact and form the hinge. The myosin neck would rotate about the hinge region to generate a 6 nm powerstroke. Following the powerstroke, actin and myosin remain strongly bound in a rigor-like conformation that is broken by the addition of ATP (Smith and Rayment, 1995).

A fundamental question remains unanswered by the model (Eisenberg and Hill, 1985): What is the energy source ultimately responsible for movement? Although the free energy available from the hydrolysis of ATP is harnessed by myosin, the hydrolysis step occurs when the motor is disengaged from actin while the force generating step occurs subsequently when actin and myosin are

tightly bound. It has been suggested that the energy driving the powerstroke comes from the formation of the strong bond between actin and myosin. As the cleft closes, the hydrophobic patches lining the upper and lower walls of the cleft are shielded from the solvent (Rayment et al., 1995b). It is believed that by burying these hydrophobic regions, the molecule is able to generate enough energy to trigger the conformational movements of different domains that act together to produce a global change in the structure of the protein (Lesk and Chothia, 1984).

High Resolution Recordings of Myosin Movement

Force-Displacement-Compliance

Recent advancements in quantitative in vitro motility assays have provided insight into the issue of myosin step-size (Ishijima et al., 1994; Finer et al., 1994). Step-size is the term used to specify the length of the powerstroke. That is, the distance that myosin moves along an actin filament following one cycle of ATP hydrolysis. Prior to the development of this technology, a wide range of estimates on myosin step-size had been reported. Until recently, some groups had reported "a giant step for myosin" (Sellers and Homsher, 1991), but presently the consensus seems to be in favor of "one small step for myosin..." (reviewed by Block, 1995). These discrepancies have been due to a large extent on differences in the experimental approach used to measure the mechanical details of myosin function. The first attempts at estimating myosin step-size used skeletal muscle fibers (Burton, 1992; Bagshaw, 1993), but these measurements were indirect in that the number of force generating myosins interacting with actin was indefinite. The first motility assays consisted of myosin-coated beads that were shown to undergo ATP-dependent movement along the polarized actin

cables of *Nitella* (Sheetz and Spudich, 1983). Subsequently, it was shown that actin filaments were translocated when placed over a myosin-coated planar surface (Kron and Spudich, 1986). This assay was used to show that S1 was sufficient to generate movement and subsequently, by attaching the actin filament to a glass needle to measure the force produced by S1 (Toyoshima et al., 1987; Kishino and Yanagida, 1988).

Recently, two new and exciting approaches to in vitro motility assays have allowed investigators to measure the force and displacement (i.e. step-size) generated by single myosin molecules within a millisecond timeframe. One approach used myosin filaments prepared from intact myosin molecules and myosin tail domains, devoid of the head region, in order to minimize the number of heads actively involved in force generation (Ishijima et al., 1994). These thick filaments were adsorbed onto a glass surface and an actin filament that had been attached at one end to an extremely fine glass needle was placed over them (see figure 6). The force and displacement produced by myosin was measured using a photodiode detector to track the position of the needle as it was bent. The position and stiffness of the needle were carefully calibrated. To mimic maximal load conditions, a stiff needle was used in the assay to show that myosin can generate 5-6 pN forces and step-sizes of 4-5 nm at the specified settings. The assay was performed with a more compliant needle to simulate lower load conditions and the step-size measured ranged from 12-22 nm at these lower loads. The diagram in figure 6 illustrates how the needle-based assayed was engineered.

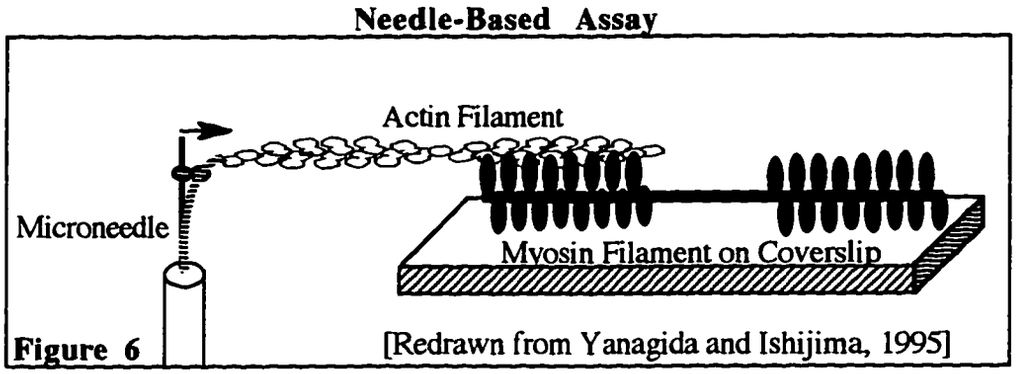

Figure 6

The other approach used HMM fragments of myosin that had been adsorbed at low concentrations onto 1 μM diameter silica beads (Finer et al., 1994). The beads were attached to a glass surface and data was collected at the lowest head densities able to support movement. Using optical traps, two 1 μM diameter beads coated with N-ethylmaleimide-modified myosin were attached to the two ends of an actin filament. Once an actin filament was trapped by the two beads at opposite ends, the beads were pulled apart to hold the actin filament under tension. The filament was placed over the HMM-coated silica beads to initiate contact. The low HMM concentration and the spherical nature of the beads provided a limit to the number of myosins binding in the plane of the actin filament. In this fashion, approximately a single HMM molecule on the bead's surface could interact with the actin filament hovering over it. The other bound HMM fragments were physically unable to stretch far enough to make any productive contacts with actin (see figure 7). Displacement was measured by monitoring the position of either bead attached to the actin filament ends using a photodiode detector. Force estimates were ingeniously measured by using the optical tweezer as a feedback-enhanced laser trap. In this design, the photodiode would counteract the force exerted by the HMM fragment on the actin filament by

applying an equal and opposite force on one of the beads attached to the filament ends. The opposing force was generated at millisecond intervals to prevent movement of the bead. Unlike the previous approach, this technique measured force under truely isometric conditions. When muscle contracts isometrically, it supports a load in a constant position. Isotonic contractions occur when the load on the muscle is constant, but the muscle changes the position of the load as it shortens (Rawn, 1989; Bagshaw, 1993). Isometric conditions provide more conclusive data on maximum force. The length of the powerstroke as measured using the laser-trap approach averaged 12 nm and the force generated by HMM was 3-7 pN.

Laser Trap Assay

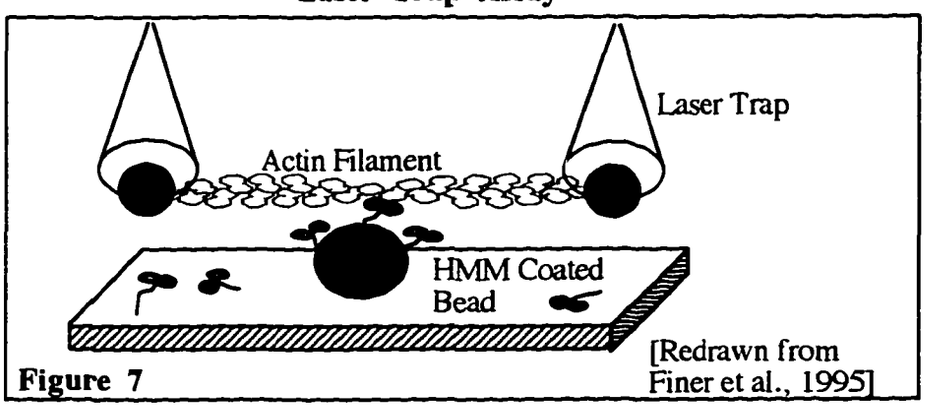

Figure 7

Compliance has become an issue of concern in these high resolution studies of motor function (Block and Svoboda, 1995). The two strands of the polypeptide that link the subdomains of the actin monomer allow the potential for relative movements of the domains. The actin filament is an extendible protein polymer assembled from multi-domained subunits (Sheterline and Sparrow, 1994). The filament can be stretched like a rubber band without breaking the intermonomer bonds since rotations about hinges between domains within the

monomers are possible. Collectively, these domain movements can lead to a change in the length of the polymer (Schutt and Lindberg, 1992). If the filament is not under tension, the myosin powerstroke will extend the filament as it is translocated. This can lead to an underestimation of the step-size. The needle -based assay creates this problem because the actin filament may not be fully extended when the movements are recorded. In the laser-enhanced optical trap system, the problem of compliance also applies since the geometric orientation of the myosin on the silica beads is unknown. It is conceivable that the motor may swivel freely and add to the compliance of the system. The degree of freedom in the rotation of the motor depends on how the myosin is bound onto the bead. Since there is variability in the geometry of attachment there is variability in the step-size measured.

Assay Improvements: Meticulous or Trivial?

One central question left unanswered by the assays described above is whether two heads are better than one. The possibility exists that the two heads of myosin or HMM may act together, each contributing a 6 nm step. In the case of other motors such as kinesin, the heads seem to act together in a cooperative fashion (Schnapp, 1995). In order to address this question for myosin, Molloy and co-workers designed a laser trap system in much the same manner as described above to test the force and displacement generated by S1 in comparison to HMM. Unlike the original laser trap assay though, the laser beam was split to make two laser traps that would track the movement of both beads attached at each end of the actin filament. These investigators argue that the single optical trap method could lead to overestimates. One of the greatest obstacles in measuring displacements in the nanometer distance range is brownian motion

(reviewed by Block, 1995). The powerstrokes generated by myosin provide signal peaks slightly above a high background of noise that must be filtered. The background noise levels that result from brownian motion are roughly the same order of magnitude as the myosin powered movement. In the optical trap method for measuring myosin step-size, the pre-tensioned actin filament and the two beads glued onto its ends continually oscillate due to thermal fluctuations. It is not difficult to envision a powerstroke and a fluctuation acting simultaneously on the actin filament to push it in the same direction. This additive effect would result in overestimated step-size measurements. There are instances when the powerstroke and fluctuations oppose each other and the net movement would be undetected above the noise or may even be negative. Therefore, the data gathered in the original laser trap assays was biased and ignored those powerstrokes that seemed to produce zero movement. The new assay used a variance-based approach to incorporate both positive and negative displacement data. The overestimated positive displacements could be easily monitored by eye since these occured clearly above the background noise. The negative or zero displacements posed a greater challenge to record. The key to detecting these relied on differentiating between zero displacements due to the mutual cancellation of opposing forces and zero displacements resulting from a disengaged myosin unable to generate a powerstroke. The binding of myosin adds rigidity to the system and creates variance over the total range of bead displacements. If myosin is disengaged from the dumbbell-shaped actin filament, then the overall noise level is higher than when myosin is bound. By switching to less filtered conditions (in which the laser traps held the actin filament less rigidly) in between peaks, Molloy and colleagues were able to calculate the noise variance over time

against more filtered readings. In between the positive displacement peaks, the investigators were able to determine if myosin was bound and attempting to move the actin filament against the thermal fluctuations acting to push the filament in the other direction. A myosin step-size of 4 nm and a force of 1.7 pN was measured for both S1 and HMM. This study does not resolve the problem of compliance in the system that results from the variability in the angular orientation of the heads on the bead. Although these and other factors (Block and Svoboda, 1995) affecting step-size estimates are important from a technical perspective, the difference between estimates seems trivial in that the various reports all argue for a short step-size of 5-12 nm that agrees well with the structural data and results from other experimental approaches (Rayment and Holden, 1994; Pate et al., 1993). Interestingly, Huxley and Simmons (1971) proposed a step-size of approximately 12 nm for myosin based on a study dealing with tension recovery after rapid shortening of an isometric muscle fiber that was done over 20 years ago. This estimate was calculated by dividing the shortening distance of the fiber by the estimated number of myosin heads actively bound.

Work-Efficiency-Duty Ratio

If myosin applies a force of 4 pN on actin over a 12 nm distance then it generates 5 x 10^{-20} Joules of work. The free energy available from the hydrolysis of ATP is close to 8.3 x 10^{-20} Joules. Therefore, myosin can use 50% of the free energy available from ATP hydrolysis to generate mechanical work. The most efficient automobile engine uses 30% of the free energy available from fuel combustion (reviewed by Cooke, 1995).

Another area of interest is the duration of the force-generating step or

strongly-bound state. Finer et al. (1994) and Ishijima et al. (1994) report different values of 7 ms and 20 ms respectively, for the duration of the strongly -bound state (Ts). Kinetic studies suggest a value of 2ms for Ts. The duty ratio is the percentage of the total ATPase cycle time (Tc) that a motor enzyme spends in the strongly-bound state (Ts) (reviewed by Spudich, 1994). Tc is approximately 50 ms for skeletal muscle myosin and considering an average value of 10 ms for Ts, the duty ratio of the motor (Ts/Tc) is about 20%. In contrast, a duty ratio of 85-90% has been calculated for the microtubule-based motor, kinesin (Kuo and Sheetz, 1993; Svoboda and Block, 1994). These values are significant because a high duty ratio is characteristic of a processive motor. A single kinesin can translocate microtubules over a 0.01 mm distance without dissociating from its tubulin-polymer substrate (Vale, 1994). RNA polymerase, the most powerful motor protein to date (Yin et al., 1995), can travel continuously along megabase distances of DNA without disengaging from its track. The low duty ratio characteristic of skeletal muscle myosin is not well suited for processive motors. The molecule would not function efficiently as a cytoplasmic motor. Since skeletal muscle myosin (myosin II) spends most of its ATPase cycle time disengaged from the actin polymer, brownian motion would cause the motor to diffuse laterally off its track. The non-processive nature of the motor works well in muscle because myosin II forms bipolar filaments that anchor it to prevent its diffusion. Other myosin isoforms (I, III-XI) must operate as processive motors in order to perform the vesicle carrier and other functions that have been proposed for them within the cytosol (See reviews by Titus, 1993; Vale, 1994; Mooseker and Cheney, 1995).

Reservations Concerning Present View of Myosin Function

Surprisingly, the exact link between ATP hydrolysis and myosin-powered movement has yet to be elucidated. The aforementioned conclusions were made without a direct measurement of ATP hydrolysis or a clear understanding of how the chemical and mechanical cycles are related. At high velocities, a number of myosin motor domains are mechanically disengaged from actin without the need for ADP/ATP exchange. It has been speculated that bypassing the nucleotide exchange step reduces the total ATPase cycle time in rapidly contracting muscle fibers (Cooke et al., 1994). In this model, ADP-bound myosin would be detached from actin by the mechanical strain resulting from the powerstroke rather than by the binding of ATP. Following detachment ADP-bound myosin would bind phosphate and subsequently generate a powerstroke following hydrolysis. Unfortunately, the ATPase activity of single myosin molecules has not been measured in conjunction with force measurements. Such data would strengthen the current assumption that the hydrolysis of ATP and the generation of movement are tightly coupled. A few groups are beginning to tackle this issue using various approaches such as the use fluorescent nucleotide analogs and high resolution microscopic techniques (Sowerby et al., 1993, Astumian and Bier, 1995). Some argue that such a deterministic picture of coupling may not be adequate to explain the behavior of actin-based motors and propose other models for how myosin works. One of these models predicts that myosin moves along actin by biased diffusion. The motor may behave as a thermal rachet to transform thermal fluctuations into unidirectional movement by using the energy available from ATP hydrolysis (Maddox, 1994; Astumian and Bier, 1994). Others contend that it is not a myosin powerstroke but instead an actin powerstroke that

generates movement and that the basis of force production lies in actin filament length changes along the direction of movement (Schutt and Lindberg, 1993). If such mechanisms apply to the way actin and myosin function, then much remains to be learned. But, clearly structural and high resolution microscopic data has provided some insight into how myosin and actin may interact. Mutagenic and biochemical approaches are starting to unravel the role of other components in the interaction and as new models are explored, investigators may yet stumble on the exact mechanism by which actin and myosin interact to generate both unidirectional displacement and force.

OBJECTIVE

Because actin and myosin interact to form a contractile, force generating system, the presence of one of these components in a subcellular localization invariably leads to speculation about the existence of the other. The presence of actin in *Tetrahymena* was questioned until Cupples and Pearlman (1986) and Hirono et al. (1987) reported a single copy gene sequence for the *Tetrahymena* actin gene. The deduced amino acid sequence for *Tetrahymena* actin showed that it has only 75% homology with other actins. Characterization of actin purified from acetone powders of total *Tetrahymena* protein revealed that, unlike other actins, *Tetrahymena* actin did not bind DNase I or phalloidin (Hirono et al., 1990). *Tetrahymena* actin localizes to various cytoskeletal components, but most notably to basal-body associated fibrillar structures in the *Tetrahymena* cortex (Metenier, 1984; Hirono et al., 1987b; Hoey and Gavin, 1992).

Identification of the gene encoding actin in *Tetrahymena* and the localization of the actin protein to cytoskeletal fibrillar structures raised immediate speculation about the existence of myosin in this organism. Despite the widespread distribution of unconventional myosins among vertebrates, invertebrates, and plants, the identification of actin-based motors in ciliates had not been described at the time this dissertation study was initiated. The objective of this study was to identify myosins in *Tetrahymena* by using biochemical, immunochemical and PCR-based approaches.

I. IMMUNOCHEMICAL AND BIOCHEMICAL EVIDENCE FOR MYOSIN IN *TETRAHYMENA*

Experimental Design

In light of the localization of actin in *Tetrahymena*, it seemed probable that myosin isoforms would co-localize with actin to cytoskeletal structures. Our approach involved the production of anti-myosin antibodies to detect putative myosins in *Tetrahymena* cytoskeletal fractions and assaying the detected proteins for myosin biochemical properties. This work has recently been published and is be summarized below (Garcés et al., 1995).

Results and Discussion

Immunochemical Evidence for Myosin in *Tetrahymena*

A rabbit antiserum was raised against a *Tetrahymena* cytoskeletal protein fraction, and anti-myosin heavy chain (MHC) antibodies were affinity-purified from the antiserum. Western blot analysis with the affinity-purified anti-MHC antibody showed that it detected a 180 kDa *Tetrahymena* cytoskeletal polypeptide. In control experiments using antigen-adsorbed antibody or preimmune serum, the 180 kDa polypeptide was not detected. The affinity purified anti-MHC antibody co-immunoprecipitated the 180 kDa protein and a putative myosin light chain of 17-18 kDa. An antibody capture assay based on antigen competition was used to quantitate the amount of the 180 kDa polypeptide in *Tetrahymena*. Based on this assay, the amount of the 180 kDa polypeptide was 33 μg/10^7 cells or 0.22% of the total cell protein.

Indirect immunofluorescence microscopy was used to localize the affinity-purified anti-MHC antibodies in *Tetrahymena*. The antibody localized to basal

bodies in the longitudinal cortical rows and in the oral apparatus, which is a feeding complex in *Tetrahymena*. There was in addition, diffuse staining of the cytoplasm and the macronucleus. Immunogold electron microscopy was used to localize the affinity-purified anti-MHC to the basal body cage complex. The antibody was closely associated with filaments which decorate the basal body surface.

Localization of p-180 to other organelles

Using a labeling strategy similar to that used for the localization of p-180 to cytoskeletal components, we have probed other cell constituents for the presence of p-180. Both immunofluorescence and immunogold labeling experiments have indicated the localization of p-180 to the nucleus and secretory organelles called mucocysts (see figures 8 and 9). The labeling pattern is similar to that seen for actin in these organelles. Myosins have been found to associate with the nuclear envelop in higher eukaryotic cells (Berrios and Fisher, 1986), but at electron microscope resolution, p-180 localizes to chromatin rich structures in the macro-nucleus and not as prominently to the nucleoplasm or nuclear envelop.

Biochemical Evidence for Myosin in *Tetrahymena*

In order to provide further evidence that the 180 kDa is a myosin, we evaluated the ATPase activity of ATP-solubilized *Tetrahymena* proteins and investigated the binding of the 180 kDa to F-actin. Most myosins exhibit a low Mg^{2+}, ATPase activity that is stimulated by F-actin under conditions of low salt concentration, and a high K^+ - EDTA, ATPase activity under conditions of high salt concentration. Both K^+ - EDTA and Mg^{2+} ATPase assays were used to measure the activity in extracts prepared by solubilization of cytoskeletal proteins

in salt solutions with and without ATP. The K^+- EDTA, ATPase activity in extracted cytoskeletal proteins was enriched approximately 5-fold when 5 mM ATP was added to the extraction solution. In the absence of F-actin, the Mg^{2+} ATPase activity was 3 nmoles Pi/mg protein/min. However, it was stimulated approximately 7-fold in the presence of F-actin. The F-actin, Mg^{2+} ATPase activity in extracts that had been depleted of the 180 kDa polypeptide by immunoprecipitation showed an 88% decrease in F-actin, Mg^{2+} ATPase activity compared with the control value. This is further evidence that the 180 kDa is a myosin heavy chain. The absence of complete inhibition of F-actin, Mg^{2+} ATPase activity in ATP-solubilized proteins that do not contain the 180 kDa polypeptide indicates additional myosins may be present in the fraction.

Another property of myosins is their ability to associate with actin filaments in an ATP-sensitive manner. In order to determine whether the 180 kDa *Tetrahymena* polypeptide displayed this property, we carried out actin cosedimentation assays using ATP-solubilized cytoskeletal proteins and actin filaments purified from skeletal muscle. ATP-solubilized proteins were mixed with phalloidin-stabilized actin filaments, incubated at 20°C with or without ATP and centrifuged at 416,000 *g*. The supernatant and pellets were analyzed by SDS-PAGE and by immunoblotting. In the absence of ATP, the 180 kDa polypeptide was shown to bind and pellet with actin. In the presence of ATP, the 180 kDa polypeptide was detected in the supernatant and not in the actin pellet .

In addition to their ability to bind actin, myosins can cross-link actin filaments in an ATP-dependent fashion. Low speed cosedimentation assays were

used to test the ability of the 180 kDa protein to bundle actin. Low speed centrifugation sediments actin filaments only when these are bundled (Pollard, 1982). We utilized the measurement of protein concentration at the meniscus before and after low speed centrifugation as a measure of actin sedimentation in assays with ATP-solubilized cytoskeletal proteins. In actin cosedimentation assays with ATP-solubilized proteins and ATP, the protein content at the meniscus decreased 3% after low speed centrifugation. When ATP was omitted from the assay, the protein content at the meniscus decreased 58% after low speed centrifugation. In the assay without ATP, low speed centrifugation pellets contained actin filaments which were organized into very dense and interconnected bundles that were visible by fluorescence microscopy when labeled with FITC-phalloidin. ATP-solubilized proteins that had been immunodepleted of the 180 kDa polypeptide were also used in a cosedimentation assay without ATP. In this assay, the protein content at the meniscus decreased by only 8% after low speed centrifugation. To show that the decrease in protein concentration resulted from immunodepletion of the 180 kDa protein and not other ATP-solubilized components, the ATP-extracted cytoskeletal fraction was put through a mock immunoprecipitation with preimmune serum instead of primary antibody and used in a control cosedimentation assay without ATP. In the control assay, the protein content at the meniscus decreased by 60% after low speed centrifugation.

Functions for p-180

A previous study of the *Tetrahymena* cytoskeleton demonstrated that a fibrillar cage which surrounds each basal body is connected to basal body microtubules by a meshwork of actin filaments (Hoey and Gavin, 1992). The

function of the actin filaments in the cage complex is unknown. One possibility is that an actomyosin contractile system in the cage complex could change the orientation of basal bodies and thereby influence the direction of ciliary motion (Hoey and Gavin, 1992). The basal body cage as a regulator of basal body position defines a potentially pivotal role for the basal body in cell motility. If *Tetrahymena* actin has a contractile function in the basal body cage complex, a myosin motor must be present. The current results strengthen the case for a myosin motor within the basal body-cage complex and provide further evidence to support our model for a contractile system within the cage complex. To our knowledge, this is the first report of a myosin protein in *Tetrahymena.*

In designing a working model to account for basal body reorientation, certain assumptions must be made. First, the filaments seen on micrographs are assumed to represent a pair of antiparallel, overlapping, bipolar filaments. Myosins may localize at the overlapping regions and therefore give the impression of a single continuous filament extending from the cage wall (CW) to the basal body wall (BBW). One filament in the actin pair would be anchored at the plus end to the CW with its minus end facing the BBW. The second is thought to attach to the BBW with its minus end facing the CW. The CW has a high electron density which is enriched by its associations and interconnections to other cytokeletal components. The rigid interwoven fibers composing the CW render it unyielding to any contractile activity. On the other hand, the basal body walls are composed of microtubules which share the "bending" capacity of ciliary (axonemal) microtubules (see figure 10). In addition, the system must be set up to allow for the differential regulation of motor function. The contractile event must be coordinated to optimize reorientation by enabling all the active myosins

along the length of one side to exert their force uniformly while deactivating the (passive) motors on the other. The side containing the actively engaged myosins would dictate the direction of the bend. It would be premature to speculate on the biochemical nature of such regulation without first characterizing other cage components.

Recently, a class I myosin has been implicated in the adaptation of hair cells in the inner ear to sustained stimulation. Hair cells respond to mechanical stimulation (sound waves) by deflecting a mechanoreceptive hair bundle. A 120 kD protein related to myosin-Iß localizes to the distal portions of the hair bundles within the sensory hair cells of the frog sacculus (Gillespie et al., 1993). The actin-based motor is found in close proximity to calcium channels within the hair bundle membrane. It has been suggested that these mechanoelectrical transduction channels are regulated mechanochemically by myosin. Mechanical shifts mediated by myosin within the hair bundle reset the positional sensitivity of a hair cell to sustained stimulation (Assad and Corey, 1992; Hudspeth and Gillespie, 1994; Solc et al., 1994). It has been speculated that brush border myosin I may function to mechanochemically regulate the transport of solute (vitamin D-dependent Ca+ uptake) through the membrane. Similarly, the 180 kDa *Tetrahymena* myosin may serve to regulate the exchange of solute across the membrane by modulating ion channels located in the proximity of basal bodies.

The localization of p-180 to mucocysts and the nucleus suggests that it may function in transporting secretory organelles (mucocysts) along actin tracks from their site of synthesis to the plasma membrane and perhaps as control elements in nucleocytoplasmic transport.

It is not clear whether or not the p-180 kDa myosin plays a role in cytokinesis

in *Tetrahymena*.

Integration of Actin Filaments With Microtubules

The mechanism by which actin filaments become integrated with basal body microtubules is unknown. One possibility is that aggregated basal body proteins function as stable nucleating sites for actin filament assembly during development of the cage complex. An *in vitro* reassembly system for the formation of basal body protein aggregates was used to evaluate this hypothesis. *Tetrahymena* basal body proteins, *in vitro*, spontaneously form dense aggregates composed of fibrillar-like elements (Gavin, 1984). We have tested the nucleation potential of reassembled basal body structures. Reassembly pellets were resuspended in actin polymerization buffer and mixed with skeletal muscle G-actin. Phalloidin was added to enhance polymerization and to stabilize newly polymerized filaments. The actin was allowed to polymerize, and the mixture was then centrifuged at 10,000 *g* which sedimented the reassembled material but did not sediment single actin filaments. Thin sections of the reassembled material were labeled with an anti-actin antibody followed by secondary antibody linked to 5 nm colloidal gold particles. Electron microscopy showed that colloidal gold particles decorated actin filaments which emerged from dense aggregated material (see figure 11). In a control experiment, reassembled material was mixed with pre-assembled actin filaments in actin polymerization buffer and sedimented at 10,000 *g*. Labeling of the reassembly aggregates by the anti-actin antibody was drastically reduced in the control preparations. In order to show that the labeled actin filaments were derived from the polymerization of exogenous G-actin, reassembly material was labeled with FITC-phalloidin which binds to vertebrate F-actin but does not bind to *Tetrahymena* actin. The reassembly aggregates were brightly fluorescent in

samples that had received G-actin, but they showed only background-level fluorescence in control samples. DNase inhibition assays were used to demonstrate that the rate of actin polymerization was higher in samples containing basal body proteins (see table 1). These results demonstrate that actin filaments can assemble onto aggregated basal body proteins which could function as stable nucleating sites for actin filaments during morphogenesis of the cage complex.

II. PCR-BASED SCREENS FOR MYOSIN IN *TETRAHYMENA*

Experimental Design

We have used a PCR-based approach to screen *Tetrahymena* genomic DNA for conserved myosin head domain sequences. Myosins have been characterized on the basis of amino acid homologies in the motor domain (Mooseker and Cheney, 1995). The head region of all but one of the known myosins is defined by a characteristic nucleotide binding site, P-loop, with the amino acid sequence GESGAGKT. A non-conserved, disordered loop (loop 1) follows the ATP-binding site (see figures 12 and 28). Loop 1 is succeeded by a conserved region located at the 25/50 kD junction which is comprised of the amino acids LEAFGNAKTV. There is another conserved amino acid region approximately 250 amino acids further towards the C-termimus of the head. The sequence for this region is G(V/I/L)DIFGFEXFE, where X stands for any amino acid. Codon bias data compiled from Martindale (1989) were used to design slightly degenerate PCR primers for these two conserved regions of sequence homology occuring downstream of the ATP-binding region within the myosin head domain (see figure 13). As shown in figure 14, a combination of two PCR techniques

(Hot Start and Touch-Down PCR, Perkin Elmer, Inc.) was used in order to minimize the mispriming events known to occur with degenerate primers and enhance the production of specific products. The PCR product was directionally cloned into an all-purpose cloning vector, pDIRECT (Clontech labs., Inc.) using a ligation independent cloning strategy. Blue/white screening was used to identify positive transformant colonies. Recombinant plasmids containing a DNA insert in the 750 bp size range were isolated and sequenced (figures 15 and 16). A deduced amino acid sequence based on the nucleotide sequence of the PCR product served to scan non-redundant databases at the National Center for Biotechnology Information (NCBI) which uses a basic local alignment search tool (BLAST) described by Altschul et al. (1990). These sequence alignments were used to detect other conserved myosin regions between the two sequences initially used in the PCR primer design. The detection of such sequences confirmed that the PCR product sequence corresponded to a partial myosin head sequence. Once it became certain that the PCR product contained sequences coding for myosin, it was desirable to obtain a larger portion of the myosin sequence with the aim of identifying the characteristic P-loop and promoting a family classification for the myosin. To accomplish this task, we employed a technique previously used for chromosome crawling known as inverse PCR (Triglia, et al., 1988). This procedure facilitates the amplification of unknown sequences flanking a target segment of genomic DNA where the nucleotide sequence is known (Ochman et al., 1988). Genomic DNA was digested with either *Eco*R 1 or *Hind* III, diluted and ligated under conditions that would favor the formation of monomeric circular template molecules (see figures 19, 21, and 24). Two oligonucleotide primers were synthesized from a region within the known PCR product sequence and

were oriented with the 3' ends directed away from each other. Amplification around the circular template resulted in a linear PCR product consisting of uncharacterized DNA fragments flanked by known myosin sequences. The inverse PCR products were T-A cloned into the vector, PCR II (Invitrogen Corp.) and subsequently sequenced (figures 23 and 26).

Results and Discussion

A 765 bp PCR product with sequence homology to known myosins

Direct sequencing with M13 and sequence-specific priming sites was used to sequence both strands of a 765 bp PCR product (figure 17). As a result of unique codon usage in ciliates, it was quite simple to assay for species cross-reactivity in the polymerase chain reactions. The 765 bp PCR product contained 9 TAA and 1 TAG codon, which in ciliates are not used as stop codons but rather as glutamine codons (Prescott, 1994). The predicted amino acid sequence of the 765 bp PCR product was aligned with known myosin head sequences using the BLAST server from the National Center for Biotechnology. Non-redundant database searches revealed that sequences in the head domain of myosin VIIA and *Arabidopsis* myosin VIII produced the highest scoring-segment pairs with the 765 bp PCR product (figure 18). The fundamental unit of the BLAST algorithm output is the high-scoring segment pair (HSP). An HSP consists of two sequence fragments of arbitrary but equal length whose alignment is locally maximal and exceeds a cutoff score. Each HSP consists of a segment from the the query sequence and one from a database sequence. BLAST programs focus on ungapped alignments. The length and number of HSP's in a search determines a p-value. The p-value is a measure of the statistical significance of an

alignment or the probability that an alignment is due to chance. Hence, the lower the probability, the greater the significance. Using the sum-statistics of the BLAST program, a p-value of 0.05 or less is significant with a 95% confidence level. The alignments between the 765 bp PCR product sequence and the myosin VII and VIII head sequences received a p-values of 10^{-60}. Based on this analysis, it was concluded that the 765 bp PCR product is a fragment of a new myosin gene with extensive homology to the myosins- VII and VIII and the first myosin gene to be discovered in ciliated protozoa.

A 3.2 kb inverse-PCR product identifies the P-loop

A 3.2 kb inverse-PCR product was generated using circularized *Eco*R 1 fragments of *Tetrahymena* genomic DNA as template (see figures 21 and 22). As illustrated in figure 20, the 765 bp PCR product sequence contained an *Eco*R 1 site approximately 480 bp from its 5 ' end. The inverse PCR primers were constructed from sequences located upstream of this restriction site. Therefore, the amplified 3.2 kb *EcoR* 1 fragment contained the first 480 bp of the 765 bp PCR product that was initially amplified with degenerate primers, and an additional 2700 bp of upstream sequences. The 3.2 kb PCR product was partially sequenced and the amino acid sequence was deduced to identify loop 1 of the *Tetrahymena* myosin gene along with several other conserved regions in the head domain. One of these regions corresponded to the unique nucleotide-binding site or P-loop shared by all myosins.

A 2.0 kb inverse-PCR product identifies a region of actin contact at the site corresponding to the 50/20 kD junction in chicken skeletal myosin II

Inverse PCR was used to amplify a 2.0 kb product from circularized *Hind* III fragments of *Tetrahymena* genomic DNA (see figures 24 and 25). The 2.0 kb

product was generated with the same primers that were used to amplify the 3.2 kb *EcoR* 1 fragment, however the primers were positioned downstream of a *Hind* III site located exactly at the 5 ' end of the 765 bp PCR product sequence (figure 20). Therefore, the 2.0 kb product included the entire 765 bp sequence (excluding the region between the primers) and approximately 1240 bp of downstream sequences. The 2.0 kb PCR product was partially sequenced and the deduced amino acid sequence revealed a high degree of homology between *Tetrahymena* myosin and myosins VII and VIII. One region of interest corresponded to loop 2 on chicken skeletal muscle myosin II located at a site of actin contact. The composition of loop 2 has been shown to influence the ATPase Activity of myosin (Uyeda et al., 1994). Although the length and sequence of loop 2 differs among myosin isoforms, its location within the head domain is defined in relation to other well conserved regions of sequence homology.

Tetmyo-1: A New Myosin Class?

As depicted in figures 27-29, a total of 2,000 bp which correspond to nearly 85% of the head region of the myosin gene in *Tetrahymena* have been sequenced and shown to match a myosin head concensus sequence that was generated from an alignment of the head domains of representatives from each of the myosin classes (Mooseker and Cheney, 1995). A sequence alignment using the BLAST program at NCBI, indicated that the *Tetrahymena* myosin is most similar to myosins-VII and -VIII based on p-values of 10^{-100} and 10^{-104}, respectively. This analysis suggests that the ciliate myosin sequence may constitute a different class of myosins that shares both myosin-VII and -VIII class-specific features. We propose the name TETMYO-1 for the first partial myosin sequence reported in *Tetrahymena thermophila* and Tetmyo-1 for the protein encoded by the

TETMYO-1 gene.

Probable Mechanism for the Regulation of Tetmyo-1

An exciting area of interest is the regulation of myosin motors. In muscle, the interaction between actin and myosin is regulated to a large extent by actin binding proteins that sterically interfere with the binding of myosin to actin (Holmes, 1995; Reinach and Farah, 1995). In these and other cellular settings, the actin-myosin interaction is regulated by the binding of Ca^{2+} to members of the EF hand family of proteins (Wolenski, 1995; Reinach and Farah, 1995). Studies on the differential regulation of myosins by phosphorylation of the head (Brzeska et al., 1989), tail (Collins et al., 1982) or the light chains (Tan et al., 1992) has recently become a subject of interest.

Myosins-I from the protozoa *Acanthamoeba castellanii* and *Dictyostelium discoideum* share the requirement for phosphorylation at the head for actin-activated ATPase activity and actin-based movement. Metazoan myosins-I and myosins-II from all other organisms, both metazoan and protozoan, are functional in the absence of head phosphorylation (see review by Bement and Mooseker, 1995). Efforts to understand the differential criterion for head phosphorylation have centered on the region upstream and inclusive of the DALAK sequence (Brzeska et al., 1989; Tan et al., 1992). Recently, Bement and Mooseker (1995) proposed TEDS rule as a molecular rationale for the differential regulation of myosin head phosphorylation. Based on an alignment of myosin sequences in the DALAK region, they discovered that all but two myosins, contain a threonine (T), glutamate (E), aspartate (D), or serine (S) located 16 positions upstream from the start of the DALAK sequence. In myosins requiring head phosphorylation, myosins-I from protozoa, yeast and *Aspergillus*, and in myosins-VI there is a

phosphorylatable residue (T or S) at the relevant site. In contrast, myosins which are enzymatically active in the absence of head phosphorylation (but which may require phosphorylation in the tail region or in the light chains) possess either a glutamate (D) or aspartate (E) at the site of phosphorylation. It has been postulated that these myosins have overcome the requirement for phosphorylation by replacing phosphorylatable amino acid residues for acidic ones. Interestingly, the site of TEDS rule corresponds to the tip of one of the myosin surface loops that makes contact with actin (Rayment et al., 1993b).

Alignment of the TETMYO sequence in the relevant region (16 positions upstream of DALAK) has identified a threonine at the TEDS rule site for head phosphorylation (see figures 18 and 29). This distinctive feature strengthens the case that TETMYO encodes a representitive from a novel class of myosins that share a high degree of homology with class VII and VIII myosins, but unlike these myosins may be regulated by phosphorylation in the head domain. In fact, the exclusive alignment of the DALAK region against comparable regions in the database using the BLAST server revealed that TETMYO is most similar to myosins-VI in this section of the molecule.

Expression of Tetmyo-1

Preliminary studies suggest that TETMYO is expressed. RT-PCR has been used to amplify a 450 bp PCR product using *Tetrahymena* RNA and myosin-specific primers (see figure 30). Antibodies have been raised against a synthetic 15 amino acid peptide that was synthesized from a deduced amino acid sequence of a non-consensus region exclusive to TETMYO. Preliminary data from dot blots have shown that the affinity-purified antibodies cross-reacted with a *Tetrahymena* cytoskeletal antigen.

MATERIALS AND METHODS

Polymerase Chain Reaction

Slightly degenerate and approximately 40-50% A-T rich primers were designed from conserved regions in the myosin head domain. The possibility of loop structures and dimerization were analyzed using a sequence analysis program (Oligos Etc.). Primer to target melting temperatures were calculated from %GC content and using the nearest neighbor rule. A 12 nucleotide extension was incorporated into the 5' end of the upstream primer (underlined) and a 13 nucleotide extension was added to the 5' end of the downstream primer (underlined) to facilitate cloning. The forward and reverse primer sequences were:

5'-CTCGCTCGCCCAGAA(G/T)C(C/T)TTCGGTAA(T/C)GC-3', and

5'-CTGGTTCGGCCCACTCAAA(A/G)ATCTCGAA(A/T)CC-3',

respectively. The amplification reactions were performed in 100 μl volumes using the GeneAmp PCR system 2400 (Perkin Elmer). Buffer conditions were optimized using the Opti-Prime PCR optimization kit (Stratagene). A reaction containing a final concentration of 10 mM Tris-HCl (pH 9.2), 1.5 mM $MgCl_2$, 25 mM KCl and 5% DMSO was judged optimal for both yield and purity. Hot start PCR was performed by mixing the PCR components at a temperature higher than the highest annealing temperature. AmpliWax PCR gem 100 (Perkin Elmer) beads were used as a barrier between two layers consisting of different PCR components. The bottom layer consisted of the optimized buffer, dNTP mix (62.5 μM each dNTP), each primer at a final concentration of 2.0 μM and water to total 25 μl. The wax barrier was formed by melting an AmpliWax bead on top

of the bottom layer at 80^0 C for 5 min and then re-solidifying the wax by incubating the PCR tube at room temperature for 5 min. The top layer consisted of buffer, 1.0 μg *Tetrahymena* genomic DNA, 2.5 units of Taq DNA polymerase and water to total a 75 μl volume. A 2 min pre-PCR hold at 95^0 C was programmed into each PCR reaction in order to denature any contaminating protease, melt the DNA template and mix the PCR components in the top and bottom layers of the tube. The cycle parameters were 0.5' at 94^0 C, 0.75' at 60-50^0 C (- 1.0 degree/cycle), 1' at 72^0 C for 10 cycles and 0.5' at 94^0 C, 0.75' at 50^0 C, 1-1.25' at 72^0 C (+ 1.0 second/cycle) for the remaining 15 cycles. This was followed by a 10 min extension at 72^0 C. A 10 μl aliquot of the PCR reaction was analyzed on a 2% agarose gel which resolved a 765 bp product.

PCR Product Purification

PCR products were purified by either of two methods. One involved resolving a product mixture by electrophoresis followed by gel purification. In this procedure, agarose gel slices (330 mg) were excised from a TAE agarose gel containing the band of interest. The DNA was purified using the Wizard PCR preps DNA purification system (Promega Corp.) following the manufacturers recommendations. Alternatively, PCR products to be cloned were purified by gel filtration chromatography to remove dNTP's, unincorporated primers, *Taq* polymerase and salt using CHROMA SPIN + TE-100 Columns (Clontech Labs., Inc.).

Cloning Strategies

PCR products were cloned using two methods. T-A cloning was done using a T-A cloning kit (Invitrogen Corp.). Briefly, a seven minute extension step at 72 degrees celsius was added to the thermal cycle program to insure the addition of a single deoxyadenosine to the 3' ends of the PCR products by *Taq* polymerase. The products were then ligated at 14 degrees celsius overnight to a linearized vector, PCR II which contained single 3' deoxythymidine residues. The insert to vector molar ratio was approximately 1:1. For ligation independent cloning, the purified PCR products were treated with T4 DNA polymerase in the presence of dTTP at 37 degrees C, for 30 minutes. The 3' to 5' exonuclease activity of the enzyme removes 11 and 12 nucleotides at the respective 3' ends of the PCR products. The presence of excess amounts of dTTP ensured that the exonuclease does not remove any bases beyond the first thymidine encountered. After the initial incubation, the enzyme was denatured by heating the mixture at 75 degrees C, for 15 minutes. The distinct 5' overhangs at either end of the PCR product permit its directional cloning. Incubation of the digested PCR products for 1 hour at room temperature with the vector pDIRECT, which contained complementary 5' G-C rich overhangs, resulted in hybrids that were sufficiently stable for transformation without the need for ligation.

Bacterial Transformation

Competent DHα5 bacterial cells with a transformation efficiency of 5 x 10^6 colonies/μg pUC 19 DNA were purchased from Clontech Laboratories, Inc. A 100 μl volume of cells were thawed on ice and mixed with 2-4 μl of the hybridization mixture. After incubating the mixture on ice for 30 minutes, the

cells were heat-shocked in a 45 degree C water bath for 45 seconds. The cells were transfered back to the ice for 2 minutes. Subsequently, the cells were grown in enriched medium (SOC) for 1 hour at 37 degrees C, with vigorous agitation (230 rpm). Transformants were plated on LB-amp + X-gal + IPTG plates, grown overnight at 37 degrees C and blue/white screened the next day.

Plasmid and Genomic DNA Preparation

A DNA extraction kit (Stratagene) was used to purify *Tetrahymena* genomic DNA from approximately 10^6 cells in the presence of 100 μg/ml of pronase and 20 μg/ml of RNase. The DNA was isolated at a concentration of 3 μg/μl with a 260/280 ratio of 1.85. For plasmid isolation, bacterial cultures were grown in 5 mls of LB broth overnight. Following alkaline lysis and neutralization, the chromosomal DNA and cell wall components were precipitated and removed by centrifugation at 14,000 rpm for 10 minutes. The plasmid DNA was adsorbed onto a silica gel-based membrane in the presence of a high concentration of chaotropic salt. The bound DNA was washed, desalted and eluted in low ionic strength buffer or water (Qiagen Comp).

Inverse Polymerase Chain Reaction

A 10 μl volume of *Tetrahymena* genomic DNA (30 μg) was incubated with 30 units of either *Eco*R 1. *Hind* III or *Bam* H1 in the appropriate buffer for 1 hour at 37 degrees C, in a 50 μl total assay volume. The digestion products were purified using a gel filtration chromatography column with an exclusion limit of 1000 bp. The purified products were analysed by electrophoresis, and it was determined that the *Hind* III and *Eco*R 1digests yielded fragments of optimal size

(in the 2-3 kb range). Fragments outside this size range failed to circularize efficiently. Serial dilutions of the fragment mixtures were incubated with 6 Weiss units of FPLC pure T4 DNA ligase in 66mM Tris-HCl (pH 7.6), 6.6 mM $MgCl_2$, 0.1 mM ATP, 0.1 mM spermidine, 10 mM DTT and stabilizers. The ligation reactions were incubated for one hour at 16 degrees C. The circularized fragments were purified using a QIAquick nucleotide removal kit (Qiagen comp). Serial dilutions of this DNA were used as template for inverse PCR. In order to lower the high melting temperatures required for the denaturation of closed circular DNA, some investigators linearize the DNA at a site betwenn the primers. Instead, we used a PCR buffer containing DMSO and glycerol as cosolvents to overcome any problems with secondary structures. The primers were approximately 60% GC rich and consisted of the following sequence:

5'-CCATCGATGTAGCTATCAATGGAGGCTCC-3'

5'-CCGCGGCCGCTTGTCCAGGAAAGGGAGAGAG-3'

The sequence analysis program (Oligos Etc) predicted the formation of secondary loop structures in each primer with melting temperatures of 39 degrees. This did not present a serious problem because the annealing temperature used was 65 degrees. For inverse PCR, a Hot-Start approach was also used. A 40 μl total volume lower layer consisted of 14 μl of water, 12.0 μl of buffer (25 mM Tricine, pH 8.7, 85 mM KOAc, 8-10% glycerol and 2% DMSO, 5.0 μl $Mg(OAc)_2$ 1.25 mM final concentration), 1 μl primers (0.5 μM each), and 8 μl of a 10 mM dNTP blend (200 μM final concentration for each dNTP). The upper layer contained 18 μl of buffer, 1-40 μl of DNA (1 μg), 2.0 μl of r*Tth* polymerase-XL plus water to total a 60 μl volume. The r*Tth* polymerase-XL is a mixture of r*Tth* polymerase and Vent DNA polymerase (4 units r*Tth*, 0.04 units

Vent) that exhibits proofreading capabilities. The cycling parameters included a pre-PCR hold at 94^0 C for 10-15 seconds, 18 rounds of a two step PCR-cycling program where the annealing and extension steps have been combined; each cycle consisted of a denaturation step at 94^0 C for 12 seconds and an annealing/extension step at 65^0 C for 5-12 minutes, followed by 22 cycles of the same two-step process with time increments of 12 seconds per cycle added to the annealing/extension step. A final extension at 72^0 C for 10-15 minutes was used as the final step of the reaction. Inverse PCR products were purified and T-A cloned to facilitate sequencing of both strands.

Sequencing

Nucleotide sequences were determined by the method of Sanger et al. (1977). Double-stranded plasmid DNA templates were used for sequencing of the cloned insert. Approximately 5 μg of plasmid DNA was denatured by adding 0.1 volumes of 2M NaOH, 2mM EDTA and incubating at room temperature for 5 minutes. Sequencing primer was added (20 pmol) to the denaturation mixture and allowed to incubate for 30 seconds. The mixture was neutralized by adding 0.1 volumes of 3M sodium acetate (pH 4.5) and precipitated with 4 volumes of 75% ethanol. The DNA was pelleted and resuspended in water along with sequenase reaction buffer. Sequencing reactions were performed following the protocols from the Sequenase version 2.0 kit (USB). Occasionally, PRC products were sequenced directly using a 3-dNTP labeling strategy.

Antibodies

A 15 amino acid peptide with the sequence KGNQELSNLRLSQFK from N- to C-term was cross-linked to keyhole limpet hemocyanin and injected into rabbits for antibody production (Research Genetics, Inc.; Huntsville, AL). For affinity purification of antibodies, the antigen was coupled to activated agarose (Bio-Rad; Richmond, CA) which was packed into a column. Protein A-purified antiserum was put through the peptide column and anti-peptide antibodies eluted with 0.2 M glycine, pH 2.8.

RT-PCR

Total RNA was isolated from *Tetrahymena* using an RNA isolation kit (Qiagen Inc.). RT-PCR was performed using a kit (Perkin Elmer Corp). Briefly, the RNA was reverse transcribed with MuLV reverse transcriptase using a 16 oligomer dT primer in the presence of RNA inhibitors. The cDNA was used for PCR employing the same primers and buffer coditions for the generation of the 765 bp PCR product.

Homology Searches

All sequence alignments were done using the BLAST program at the National Center for Biotechnology Information (NCBI). Amino acid alignments were performed without gaps using the default paramenters of the blastp program in conjunction with a BLOSUM-62 statistical matrix function devoid of filters.

DNase Inhibition assays

Reassembly material was prepared as described by Gavin (1984). DNase

inhibition assays were performed as described by Blikstad et al. (1978). One activity unit equals 1% inhibition of DNase activity. All assays were carried out with fixed amounts of DNA, DNase and exogenous actin and incubated for 10 minutes at 37 degrees C. Percent inhibition was calculated from absorbancy values. Each activity unit is based on the average of at least two DNase activity determinations.

Table 1. Effect of Basal Body Proteins on Actin polymerization Assayed by DNase Inhibition

Assay Conditions	Activity Units
Exogenous G-actin	51
Exogenous G-actin after 1 hr polymerization	26
Exogenous G-actin + reassembly pellet after 1 hr polymerization	09
Exogenous G-actin + reassembly supernatant after 1 hr polymerization	30
Reassembly pellet + 1 hr incubation	00

DNase inhibition assays were performed as described by Blikstad et al. (1978).

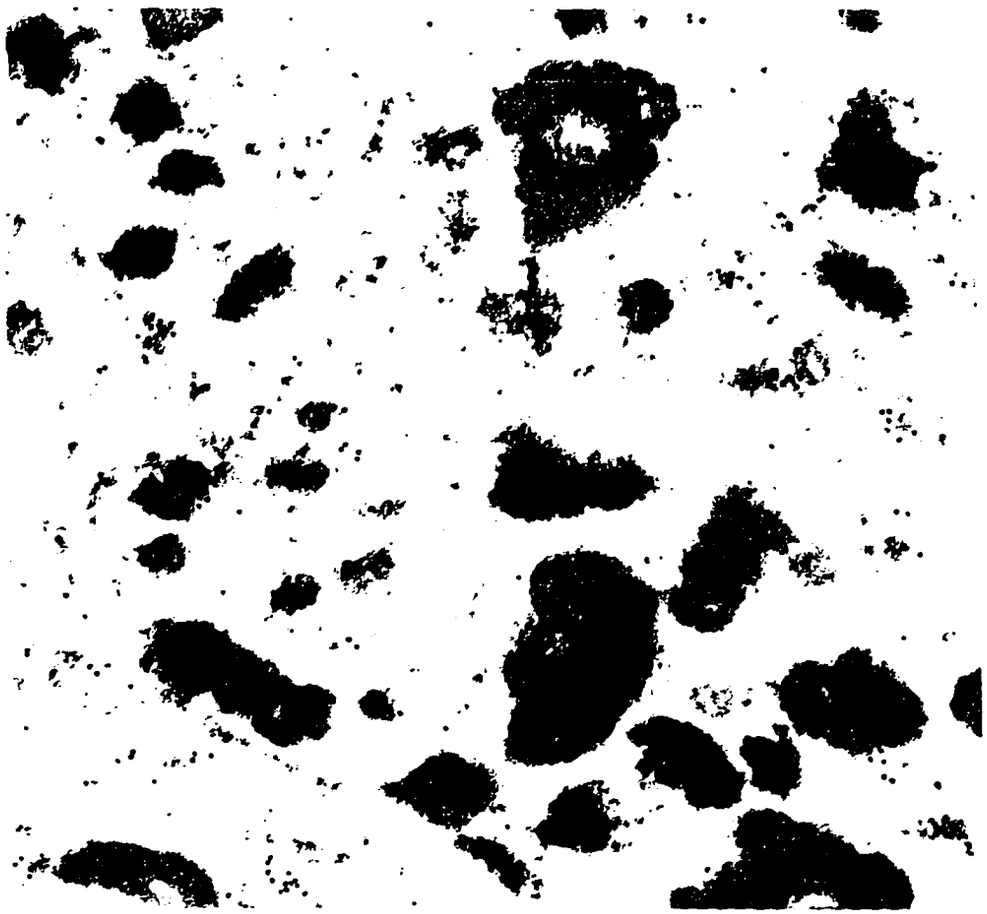

Figure 8. A cross-section through a portion of the macronucleus. The section was labeled with affinity-purified, anti-MHC antibody followed by 15 nm colloidal gold linked anti-IgG secondary antibody. Magnification scale: 1mm = 16 nm

Figure 9. Immunogold localization of p-180 to mucocysts *in situ.* The section shown was labeled with affinity-purified, anti-MHC antibody followed by secondary antibody linked to 15 nm colloidal gold particles. Magnification scale: 1mm = 8 nm.

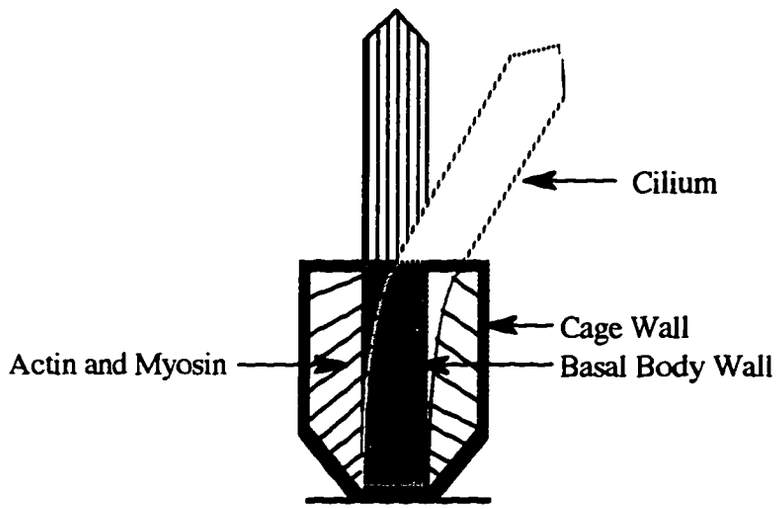

Figure 10. A cartoon representation of the basal body-cilium complex with attached filamentous cage. Microfilaments interconnect the basal body wall with the cage wall. Actin and myosin have been localized to the intracage microfilaments (contractile fibers) and are proposed to be components of a contractile system which could reorient the basal body and change the direction of ciliary movement.

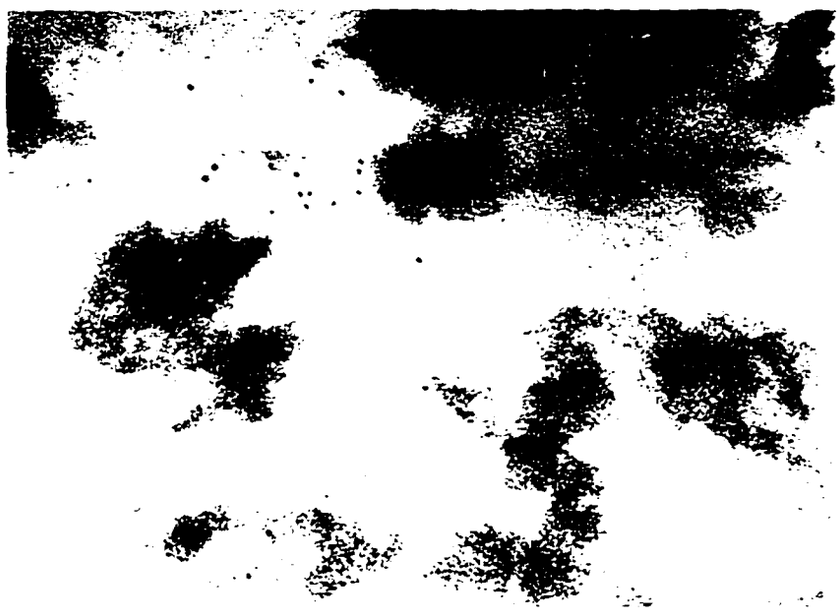

Figure 11. Immunogold localization of skeletal muscle actin filaments nucleated from basal body protein aggregates. The section shown in the micrograph was labeled with affinity-purified, anti-actin antibody followed by secondary antibody linked to 5 nm colloidal gold particles. Magnification scale: 1mm = 6 nm.

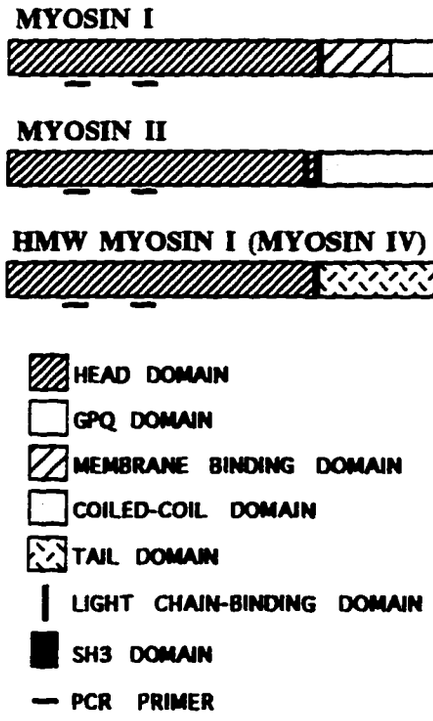

Figure 12. Diagrammatic representation of myosin head domain sequences from *Acanthamoeba* myosin I, skeletal muscle myosin II, and *Acanthamoeba* myosin IV that were aligned in search of conserved amino acid regions (LEAF and GI/VLDI) which were used in the PCR primer design.

CODON USAGE IN *TETRAHYMENA*

L	TTG	064	D	GAT	107
	CTC	062		GAC	047
	TTA	055			
	CTT	053	I	ATT	102
	CTA	009		ATC	100
	CTG	004		ATA	016
E	GAA	190	N	AAC	098
	GAG	016		AAT	047
A	GCT	165	K	AAG	249
	GCC	076		AAA	058
	GCA	009			
	GCG	000	S	TCT	083
				TCC	069
F	TTC	108		TCA	021
	TTT	027		TCG	001
				AGT	010
G	GGT	178		AGC	016
	GGA	014			
	GGC	009			
	GGG	001			

Figure 13. Codon usage data for the amino acids used in the PCR primer design. These data were compiled from Matindale (1989).

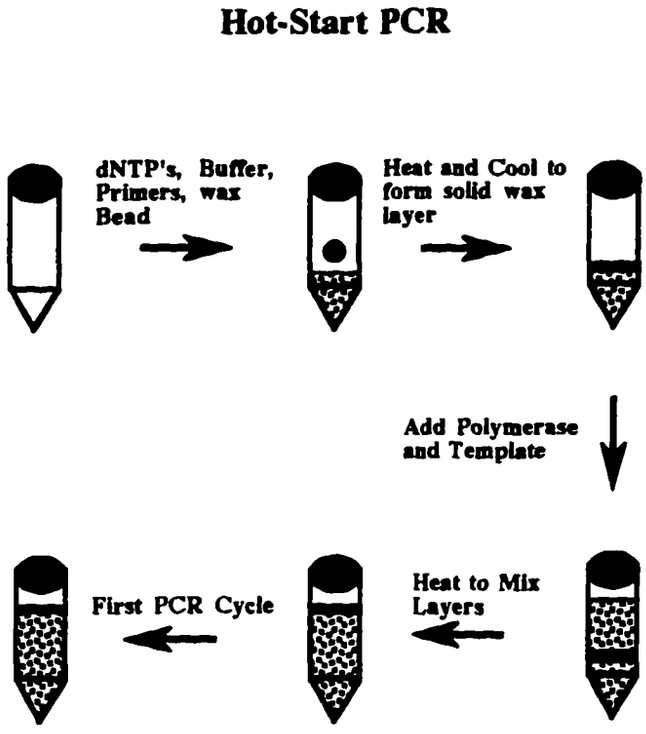

Figure 14. Schematic representation of the Hot-Start PCR technique.

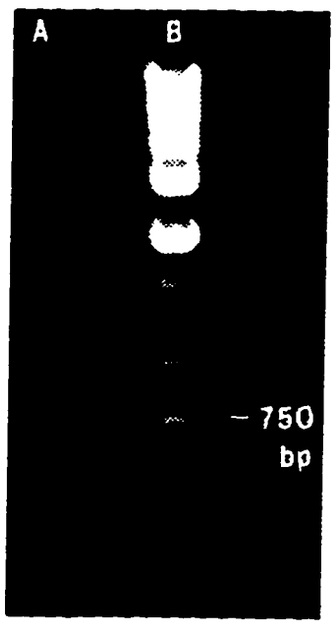

Figure 15. Photograph of a 2% agarose gel showing the 765 bp PCR product that was generated using slightly degenerate primers designed against conserved sequences in the myosin head domain in lane A, and a kb ladder in lane B.

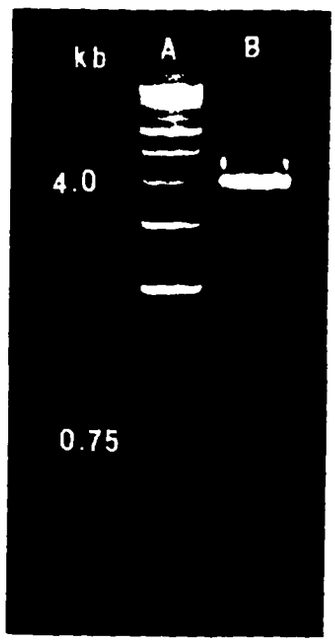

Figure 16. Photograph of a 1% agarose gel showing plasmid DNA that had been digested with *Bam* H1/*Hind* III to release the 765 bp insert (B). Lane A contains a kb ladder.

GAAG CTTTTGGTAA TGCTAAAACA
GTAAGAAATA ATAATTCCTC TAGATTTGGT
AAATACGTAA AAATCTACAT AGATAAAACA
TCTTAAAAGA TAAATGGAGC CTCCATTGAT
AGCTACTTAC TCGAAAAGAG CAGAATACCT
TGTCCAGGAA AGGGAGAGAG AAATTATCAC
ATTTTTTACC ACATGCTAAA AGGAAATCAA
GAACTATCTA ATTTGAGATT GAGTTAGTTC
AAAAATTTAT CTGATTTTGA TTATCTAAAG
AAAAGTGACT GCTTTGAGGT TGAGAACATT
TAAGATGCTA AACTCTATTT GGAAGTAAAG
AAGTCCTTCA GATAAATGAA TTTCTCTAAC
TAAGAGTAAG AAGCTATATT TTCTCTAATA
TCTGCGATAC TACTGTTAGG CAATGCAAAT
TTAGACTCAT CAAAAGTTAG CGACACTCAG
GCTCCAACTT TTTTGAACAT GAGTTTACCG
ACACATCATA AAGAATTCAA AAATGCCTCT
GAGTTACTCT AAGTTAATCC TAAAGACCTT
GAAGAGTCTT TAGTATTTAA GGTAAGGAAA
GTTGGAACTA CAGTAATTAA ATCTCCATAA
ACTGCTGAAG AATGCTTGTC TATGAGAGAC
AGTCTAAGTA AAAATCTATA TGATAGTCTT
TTTAACTTTT TGGTTTGG AA GTTAAATTAA
AATTTGTTGC CACCTTAAGA TTTGCTAAAT
AAATCATTAA GCATAGGCCT TTTAGATATA
TTTGGTTTTG AGAGCTTTGA T

Figure 17. The nucleotide sequence of the 765 bp PCR product. The letters in bold indicate a restriction site. The underlined letters correspond to the sequences used for the construction of inverse PCR primers.

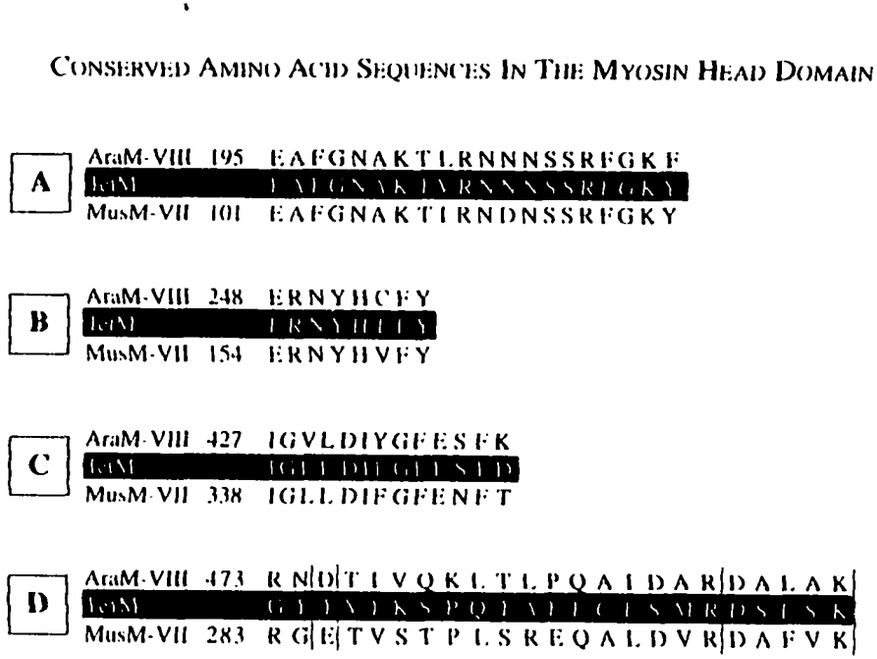

Figure 18. An alignment of the deduced amino acid sequence encoded by the 765 bp PCR product with sequences from *Arabidopsis* myosin VIII and myosin VII from mouse. (A) Region immediately downstream of LEAF. The leucine is not shown in the sequence because the codon usage for the amino acid was to degenerate to include in the primer design. (B) Conserved region located between LEAF and GILDI. (C) The GILDI region. (D) Less conserved site for head phosphorylation.

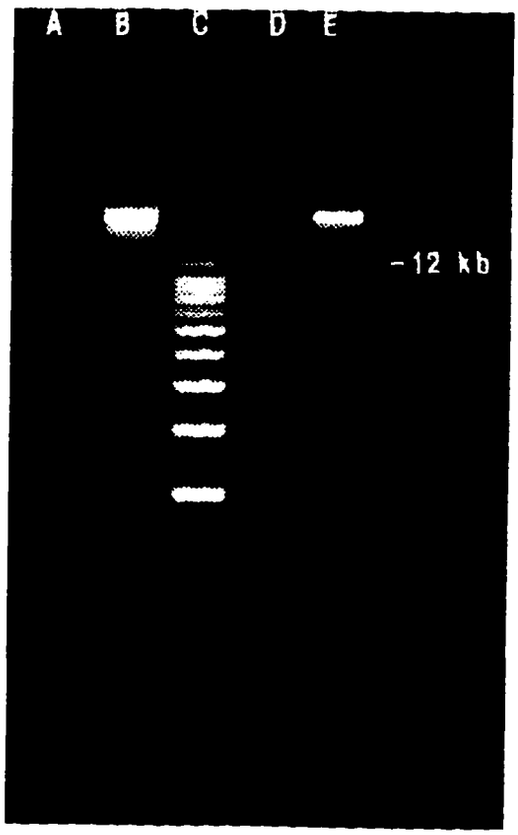

Figure 19. Photograph of a 0.8% agarose gel showing the digestion products of 20 μg of *Tetrahymena* genomic DNA following treatment with 24 units of *EcoR* 1 (A), 40 units of *Bam* H1 (B), 20 units of *Hind* III (D), and 20 units of *Bam* H1 (E). Lane C contains a kb ladder as markers.

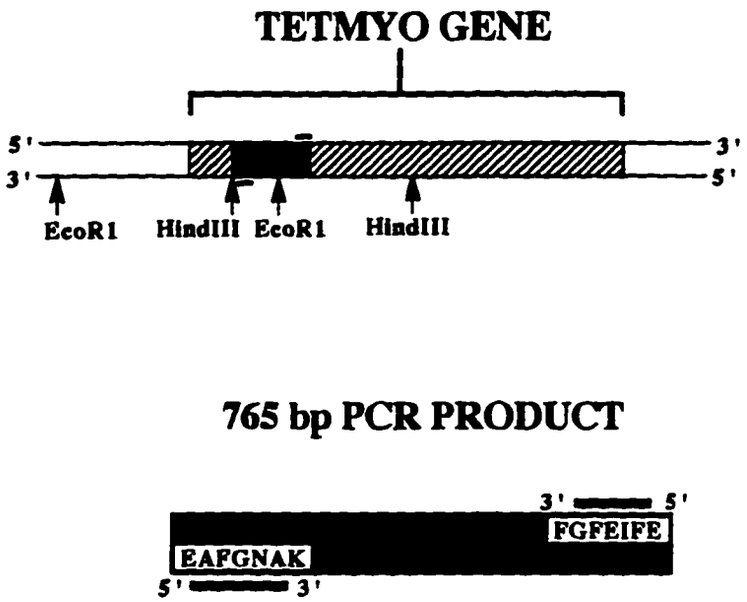

Figure 20. *EcoR* I/*Hind* III restriction map of the TETMYO-1 gene in relation to the 765 bp PCR product.

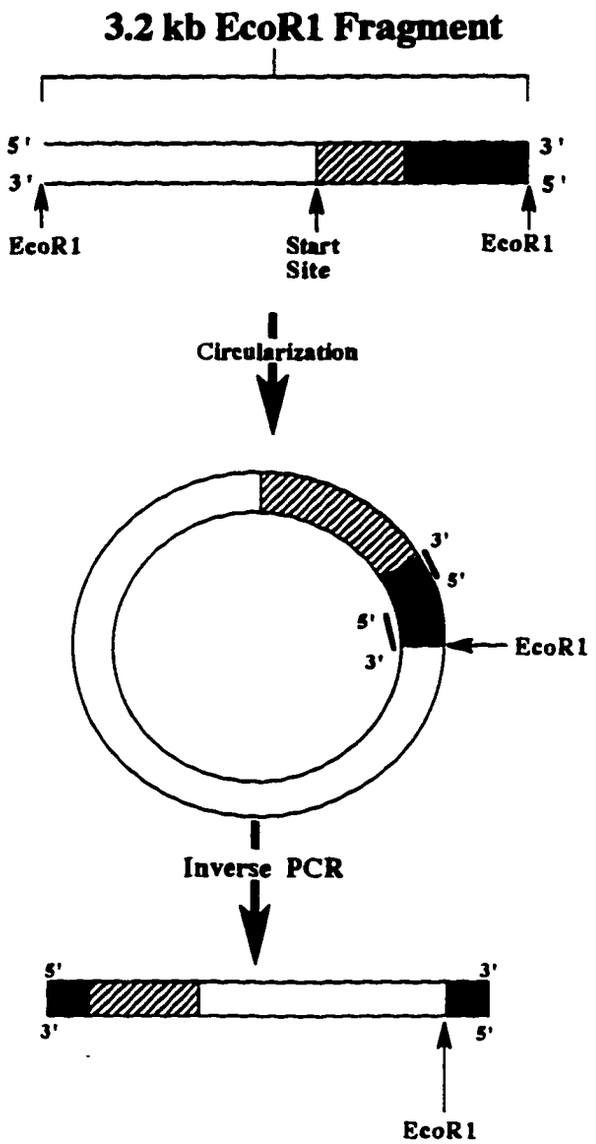

Figure 21. Diagram illustrating the inverse PCR strategy used to amplify sequences upstream of the 765 bp PCR product. The cross-hatched box represents upstream regions encoding TETMYO-1 sequences. The white box represents sequences upstream of the TETMYO-1 gene. The black box represents the 765 bp PCR product.

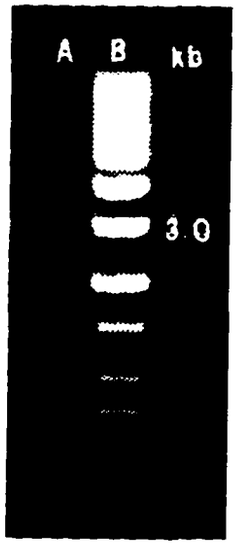

Figure 22. Photograph of a 1% agarose gel showing the 3.2 kb inverse PCR product obtained by using circularized *EcoR* 1 fragments as template (A). Lane B shows a kb ladder.

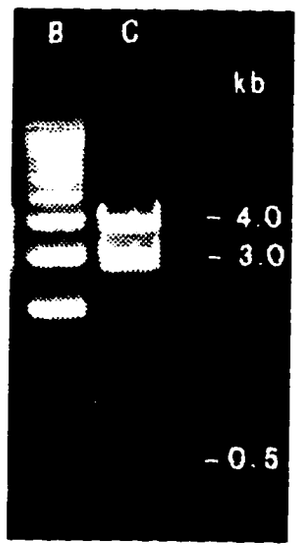

Figure 23. The 3.2 kb PCR product was T-A cloned. The gel photograph above shows a kb ladder in lane B and the digestion products of a plasmid treated with *EcoR* 1 to release the insert in lane C. The 3.2 kb insert contains an *EcoR* 1 site approximately 450 bp away from its end.

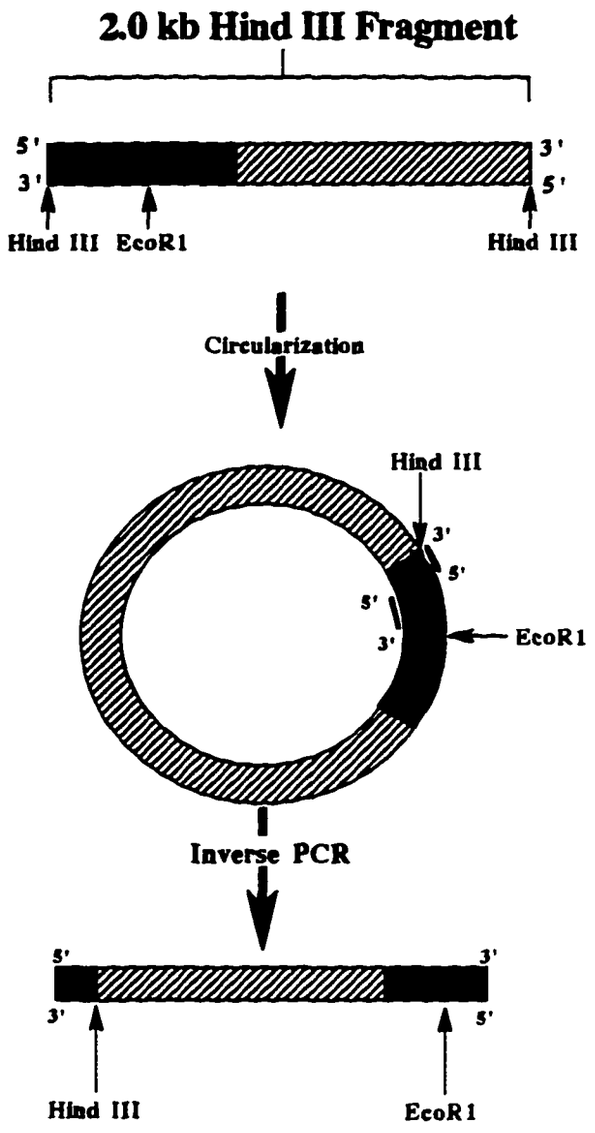

Figure 24. Inverse PCR strategy used for the amplification of sequences downstream of the 765 bp PCR product. The cross-hatched box represents downstream sequences and the black box represents the 765 bp PCR product sequence.

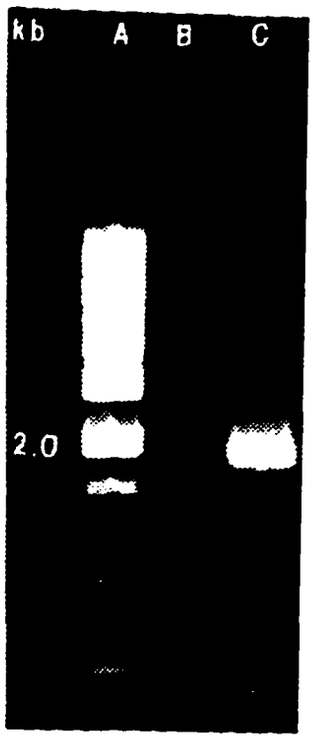

Figure 25. Photograph of a 1% agarose gel showing the amplified 2.0 kb inverse PCR product. Lane A shows a kb ladder and Lane C shows the 2.0 kb product that was amplified using circularized *Hind* III digestion fragments as template. In lane B, the digestion fragments were undiluted in the circularization reaction and resulted in no PCR product. In lane C, the digestion fragments were diluted 1:100 before circularization to optimize for intramolecular ligation over the formation of concatamers.

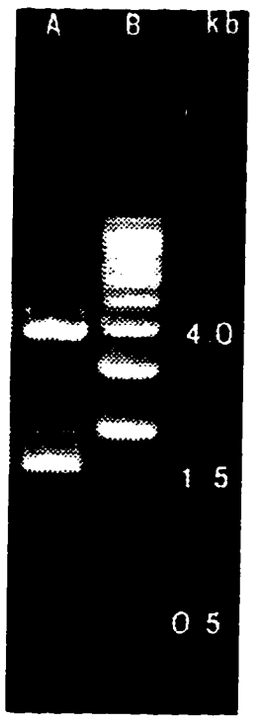

Figure 26. Photograph of a 1% agarose gel showing the T-A cloned 2.0 kb PCR product. Lane A shows the digestion products after treatment with *EcoR* 1. Lane B shows a kb ladder.

T

CTCTTCAAAC TTTAGGTTAT TCAGATATGG TTCATATGAA
GTATTTAAAT GAGGCTGAAA TAATCAATAA TTTGAGAAAG
CGATATTAAA ATAATATGAT TTTCACATAT ATTGGACCAA
CTTTGGTAGT TATGAATCCT TATAAAGAAA TAGAAGGTGT
TTAAGATAAT CAAGTAATAG ATAAAATAAA ATCTGATCTA
GGCATAAAAT TTGAAGAGGA TTTCAAAATG AATAATCTGA
GCACCAACTA AAATATTATA AACACACCTC ATACATATAC
TGTAAGCGGA TTA GCCTACA AATAAATGTT TAGCAATAAG
AAAAATTAAG CAATAGTTAT ATCAGGCGAA AGTGGAGCAG
GTAAAACGGA AAATGCTAAA TTATCGATGC AATTTTTAAC
AAGTTTGAGT TCAGGGTCTG ATAAATAAAA TGATTTACTC
AATTAATTAA AGACTCAAAC AGCTAAGAAT ATTCTATTAG
AAGAGTTTAA CTAATTTGCA ATAGAAGTAA AAATACTTGC
TTGTAATCCT ATTCTAGAAG CTTTTGGTAA TGCTAAAACA
GTAAGAAATA ATAATTCCTC TAGATTTGGT AAATACGTAA
AAATCTACAT AGATAAAACA TCTTAAAAGA TAAATGGAGC
CTCCATTGAT AGCTACTTAC TCGAAAAGAG CAGAATACCT
TGTCCAGGAA AGGGAGAGAG AAATTATCAC ATTTTTTACC
ACATGCTAAA AGGAAATCAA GAACTATCTA ATTTGAGATT
GAGTTAGTTC AAAAATTTAT CTGATTTTGA TTATCTAAAG
AAAAGTGACT GCTTTGAGGT TGAGAACATT TAAGATGCTA
AACTCTATTT GGAAGTAAAG AAGTCCTTCA GATAAATGAA
TTTCTCTAAC TAAGAGTAAG AAGCTATATT TTCTCTAATA
TCTGCGATAC TACTGTTAGG CAATGCAAAT TTAGACTCAT
CAAAAGTTAG CGACACTCAG GCTCCAACTT TTTTGAACAT
GAGTTTACCG ACACATCATA AAGAATTCAA AAATGCCTCT
GAGTTACTCT AAGTTAATCC TAAAGACCTT GAAGAGTCTT
TAGTATTTAA GGTAAGGAAA GTTGGAACTA CAGTAATTAA
ATCTCCATAA ACTGCTGAAG AATGCTTGTC TATGAGAGAC
AGTCTAAGTA AAAATCTATA TGATAGTCTT TTTAACTTTT
TGGTTTGG AA GTTAAATTAA AATTTGTTGC CACCTTAAGA
TTTGCTAAAT AAATCATTAA GCATAGGCCT TTTAGATATA
TTTGGTTTTG AGAGCTTTGA TATAAACTCA TTTGAGCAGC
TTTGCATTAA TTTTACCAAT GAAAAATTTT AGTAATTGTA
TGTTTAATAT GTTTTCAAAA GCGAAGAAGA AGATTATAAA
TAAGAAGGAA TTTTGGATGT ATTTTCTGAT TTATAATATT
AAGAGAATTA GCTCATTATT GATACAATTG AAAAAAAACC
CAATGGTAAA TTCTTATTTT CATATTTTAC ATTTTGATTT
ATATTTTATT TAAAGGAATC ATGGTGCTTT TAGATGAAAA
TTGCTCATTG GGATCAGGGA CGGATGATTC TTTTTTAAAT
TAAATTACAA AAAACCACTC TAAAAATCAA CTTGTCAGCT
TCCCTAAAAA AGATAAATAT TCTTTCAGCC TTAGTCATAC
AGCAAAACGA GTTGTATATG ATGTGCGCGG ATTTAGAGAT
AAAAATAAAG ATGAAGTAGA AAAATGTCTT TAAAGTAGTA
AATGTCCAGT TATTGCGAAT TTATTATCTT ATTAAGGCTC
TTAAACTTAG TAGAATAAAG AAACTTAAAA TCTTCAAAAT
TTTGGAAATA ATTTAAATTT TAAAAAAGTG AAATTAGTAA
TCAAA

Figure 27. The sequence of approximately 2000 bp of the TETMYO gene. The sequence represents 80% of the myosin head domain.

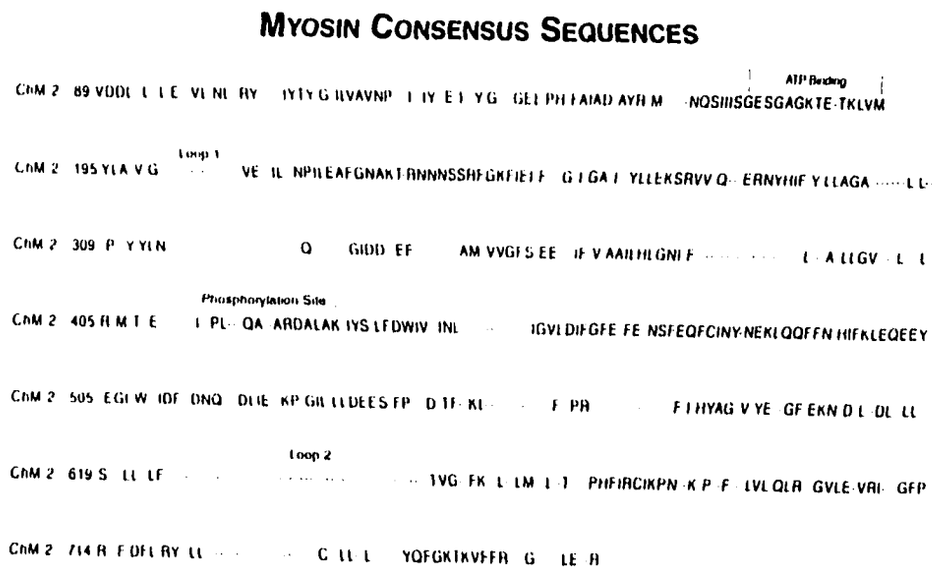

Figure 28. A myosin amino acid concensus sequence was constructed by Mooseker and Cheney (1995) from the alignment of myosin representatives in each of the 11 myosin classes. The amino acid numbers are based on the chicken myosin II sequence. The consensus sequence comprises the entire head domain of myosins.

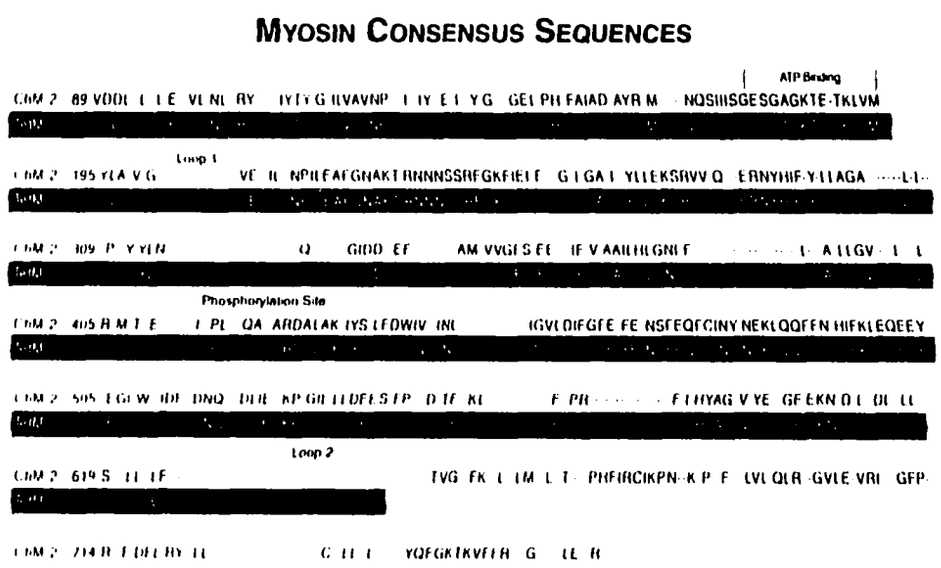

Figure 29. Alignment of the deduced amino acid sequence for Tetmyo-01 with the myosin head domain consensus sequence. Only exact matches are shown.

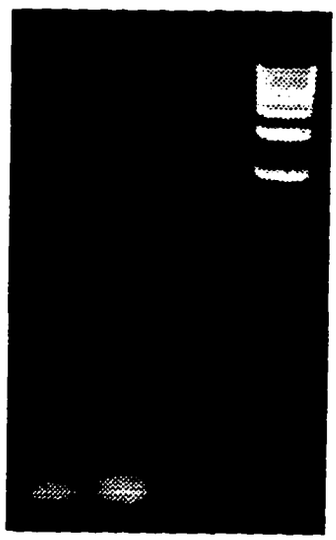

Figure 30. Photograph of a 2% agarose gel showing the product of the RT-PCR reaction. A kb ladder is shown at the far right.

BIBLIOGRAPHY

Adelstein, R. S. and Eisenberg, E. (1980). Regulation and kinetics of the actin-myosin-ATP interaction. *Annu. Rev. Biochem.* **49**, 921-956.

Altschul, S. F., Gish, W., Miller, W., Myers, E. W. and Lipman D. J. (1990). Basic local alignment search tool. *J. Mol. Biol.* **215**, 403-410.

Amos, L. A., Huxley, H.E., Holmes, K. C., Goody, R. S. and Taylor, K. A. (1982). Structural evidence that myosin heads may interact with two sites on F-actin. *Nature* **299**, 467-469.

Andreev, O. A. and Borejdo, J. (1991). The myosin head can bind two actin monomers. *Biochem. Biophys. Res. Commun.* **177**, 350-356.

Assad, J. A. and Corey, D. P. (1992). An active motor model for adaptation by vertebrate hair cells. *J. Neurosci.* **12**, 3291-3309.

Astumian, D. R. and Bier, M. (1994). Fluctuation driven rachets: molecular motors. *Phys. Rev. Lett.* **72**, 1766-1769.

Astumian, D. R. and Bier, M. (1995). Mechanochemical coupling of molecular motors to ATP hydrolysis. *Biophys. J.* **68**, 219s.

Bähler, M., Kroschewski, R., Stoffler, H. E., and Behrmann, T. (1994). Rat myr4 defines a novel subclass of myosin I: Identification, distribution, localization and mapping of calmodulin binding sites with differential calcium sensitivity. *J. Cell Biol.* **126**, 375-389.

Bähler, M. (1996). Myosins on the move to signal transduction. *Curr. Opin. Cell Biol.* **8**, 18-22.

Bagshaw, C. R. (1993). Muscle contraction. Chapman & Hall, London.

Bement, W. M., Hasson, T., Wirth, J. A., Cheney, R. E. and Mooseker, M. S. (1994). Identification and overlapping expression of multiple unconventional myosins in vertebrate cell types. *Proc. Natl. Acad. Sci. USA* **91**, 6549-6553.

Bement, W. M. and Mooseker, M. S. (1995). TEDS rule: A molecular rationale for differential regulation of myosins by phosphorylation of the heavy chain head. *Cell Motil. Cytoskel.* **31**, 87-92.

Berrios, M. and Fisher, P. A. (1986). A myosin heavy chain-like polypeptide is associated with the nuclear envelope in higher eukaryotic cells. *J. Cell Biol.* **103**, 711-724.

Blikstad, I., Markey, F., Carlsson, L., Persson, T. and Lindberg, U. (1978). Selective assay of monomeric and filamentous actin in cell extracts using

inhibition of deoxyribonuclease I. *Cell* **15**, 935-943.

Block, S. M. (1995). One small step for myosin. *Nature* **378**, 132-133.

Block, S.M. and Svoboda, K. (1995). Analysis of high resolution recordings of motor movement. *Biophys. J.* **68**, 230s-241s.

Bork, P., Sander, C. and Valencia, A. (1992). An ATPase domain common to prokaryotic cell cycle proteins, sugar kinases, actin, and hsp 70 heat shock proteins. *Proc. Natl. Acad. Sci. USA* **89**, 7290-7294.

Brockerhoff, S. E., Stevens, R. C. and Davis, T. N. (1994). The unconventional myosin, Myo2p, is a calmodulin target at sites of cell growth in *Saccharomyces cerevisiae*. *J. Cell Biol.* **124**, 315-323.

Brzesca, H., Lynch, T. J., Martin, B. and Korn E. D. (1989). The localization and sequence of the phosphorylation sites of *Acanthamoeba* myosins-I. *J. Biol. Chem.* **264**, 19340-19348.

Burton, K. (1992). Myosin step size estimates from motility assays and shortening muscle. *J. Muscle Res. Cell Motil.* **13**, 590-607.

Chen, I. L., Edwards, K, Lin, R. C.Coats, L. W. and Kiehart, D. P. (1991). *Drosophila* myosin heavy chain at 35B, C. *J. Cell Biol.* **115**, 330a (Abstract).

Cheney, R. E. and Mooseker, M. S. (1992). Unconventional myosins. *Curr. Opin. Cell Biol.* **4**, 27-35.

Cheney, R. E., Riley, M. A. and Mooseker, M. S. (1993a). Phylogenetic analysis of the myosin superfamily. *Cell Motil. Cytoskel.* **24**, 215-223.

Cheney. R. E., O' Shea, M. K., Heuser, J. E., Coelho, M. V., Wolenski, J. S., Espreafico, E. M., Forscher, P., Larson, R. E. and Mooseker, M. S. (1993b). Brain myosin-V is a two headed unconventional myosin with motor activity. *Cell* **75**, 13-23.

Collins, J. H., Cote, G. P. and Korn, E. D. (1982). Localization of the three phosphorylation sites on each heavy chain of *Acanthamoeba* myosin-II to a segment at the end of the tail. *J. Biol. Chem.* **257**, 4259-4334.

Cooke, R. (1986). The mechanism of muscle contraction. *Crit. Rev. Biochem.* **21**, 53-118.

Cooke, R. (1995). The actomyosin engine. *FASEB. J.* **9**, 636-642.

Cooke, R., White, H. and Pate, E. (1994). A model of the release of myosin heads from actin in rapidly contracting muscle fibers. *Biophys. J.* **66**, 778-788.

Cupples, C. G., Pearlman, R. E. (1986). Isolation and characterization of the actin gene from *Tetrahymena thermophila*. *Proc Natn. Acad. Sci. USA* **83**,

5160-5164.

Doberstein, S. K., Baines, I. C., Wiegand, G., Korn E. D. and Pollard, T. D. (1993). Inhibition of contractile vacuole function *in vivo* by antibodies against myosin I. *Nature* **365**, 841-844.

Eisenberg, E. and Hill, T. L. (1985). Muscle contraction and free energy transduction in biological systems. *Science* **227**, 999-1006.

Espreafico, E. M., Cheney, R. E., Matteoli, M., Nascimento, A. A. C., DeCamilli, P. V., Larson, R. E. and Mooseker, M. S. (1992). Primary structure and cellular localization of chicken brain myosin-V (p190), an unconventional myosin with calmodulin light chains. *J. Cell Biol.* **119**, 1541-1557.

Fath, K. R. and Burgess, D. R. (1993). Golgi-derived vesicles from developing epithelial cells bind actin filaments and possess myosin-I as a cytoplasmically oriented peripheral membrane protein. *J. Cell Biol.* **120**, 117-128.

Fath, K. R. and Burgess, D. R. (1994). Unconventional myosin -mediated membrane motility. *Curr. Opin. Cell Biol.* **6**, 131-136.

Finer, J. T., Simmons, R. M. and Spudich, J. A. (1994). Single myosin mechanics: picoNewton forces and nanometre steps. *Nature* **368**, 113-119.

Finer, J. T., Mehta, A. D. and Spudich, J. A. (1995). Characterization of single actin-myosin interactions. *Biophys. J.* **68**, 291s-297s.

Fisher, A. J., Smith, C. A., Thoden, J., Smith, R., Sutoh, K., Holden, H. M. and Rayment, I. (1995). Structural studies of myosin-nucleotide complexes: A revised model for the molecular basis of muscle contraction. *Biophys. J.* **68**, 19s-28s.

Fukui, Y., Lynch, T. J., Brzeska, H. and Korn, E. D. (1989). Myosin I is located at the leading edges of locomoting *Dictyostelium* amoebae. *Nature* **341**, 328-331.

Garcés, J. A. and Gavin, R. H. (1995). PCR-cloning of myosins in Tetrahymena. *Mol. Biol. Cell.* **6s**, 145a (Abstract).

Garcés, J. A., Hoey, J. G. and R. H. Gavin. (1995). Putative myosin heavy and light chains in *Tetrahymena*: Co-localization to the basal-body cage complex and association of the heavy chain with skeletal muscle actin filaments in vitro. *J. Cell Sci.* **108**, 869-881.

Gavin, R. H. (1984). In vitro reassembly of basal body components. *J. Cell Sci.* **66**, 147-154.

Geeves, M. A. (1991). The dynamics of actin and myosin association and the

cross-bridge model of muscle contraction. *Biochem. J.* **274**, 1-14.

Geeves, M. A. (1992). The actomyosin ATPase: a two-state system. *Philos. Trans. R. Soc. Lond. Ser. B. Biol. Sci.* **336**, 63-70.

Geisterfer-Lowrance, A. A. T., Kass, S., Tanigawa, G., Vosberg, H. P., McKenna, W., Seidman, C. E. and Seidman, J. G. (1990). A molecular basis for familial hypertrophic cardiomyopathy: a ß-cardiac myosin heavy chain gene missense mutation. *Cell* **62**, 999-1006.

Gibson, F., Walsh, J., Mburu, P., Valera, A., Brown, K. A., Antonio, M., Beisel, K. W., Steel, K. P. and Brown, S. D. M. (1995). A type VII myosin encoded by the mouse deafness gene shaker-1. *Nature* **374**, 62-64.

Gibson, T. J., Hyvönen, M., Musacchio, A. and Saraste. M. (1994). PH domain: the first anniversary. *Trends Biochem. Sci.* **19**, 349-353.

Gillespie, P. G., Wagner, M. C. and Hudspeth, A. J. (1993). Identification of a 120 kD hair-bundle myosin located near stereociliary tips. *Neuron* **11**, 581-594.

Goldman, Y. E. (1987). Kinetics of the actomyosin ATPase in muscle fibers. *Annu. Rev. Physiol.* **49**, 632-644.

Goodson, H. V. and Spudich, J. A. (1993). Molecular evolution of the myosin family: relationships derived from comparisons of amino acid sequences. *Proc. Natl. Acad. Sci. USA* **90**, 659-663.

Griscelli, C., Durandy, A., Guy-Grand, D., Daguillard, F., Herzog, C. and Prunieras, M. (1978). A syndrome associating partial albinism and Immunodeficiency. *Am. J. Med.* **65**, 691-702.

Haarer, B. K., Petzold, A., Lillie, S. H. and Brown. S. S. (1994). Identification of *MYO4*, a second class V myosin gene in yeast. *J. Cell Sci.* **107**,1055-1064.

Hall, A. (1994). Small GTP binding proteins and the regulation of the actin cytoskeleton. *Annu. Rev. Cell Biol.* **10**, 31-54.

Hammer, J. A. (1994). The structure and function of unconventional myosins: a review. *J. Muscle Res. Cell Motil.* **15**, 1-10.

Hasson, T. and Mooseker, M. S. (1994). Porcine myosin-VI: characterization of a new mammalian unconventional myosin. *J. Cell Biol.* **127**, 425-440.

Hasson, T., Heintzelman, M. B., Santos-Sacchi, J., Corey, D. P.and Mooseker, M. S. (1995). Expression in cochlea and retina of myosin VIIA, the gene product defective in Usher syndrome type 1B. *Proc. Natl. Acad. Sci. USA* **92**, 9815-9819.

Hirono, M., Endoh, H., Okada, N. Numata, O., Watanabe, Y. (1987a).

Tetrahymena actin. Cloning and sequencing of the *Tetrahymena* actin gene and identification of its gene product. *J. Molec. Biol.* **194**, 181-192.

Hirono, M., Nakamura, M., Tsunemoto, M., Yasuda, T., Ohba, H., Numata, O., Watanabe, Y. (1987b). *Tetrahymena* actin: Localization and possible biological roles of actin in *Tetrahymena* cells. *J. Biochem.* **102**, 537-545.

Hirono, M., Tanaka, R., Watanabe, Y. (1990). *Tetrahymena* actin: Copolymerization with skeletal muscle actin and interactions with muscle actin-binding proteins. *J. Biochem.* **107**, 32-36.

Hoey, J. G. and Gavin, R. H. (1992). Localization of actin in the *Tetrahymena* basal body-cage complex. *J. Cell. Sci.* **103**, 629-641.

Holmes, K. C., Popp, D., Gebhardt, W. and Kabsch, W. (1990). Atomic model of the actin filament. *Nature* **347**, 44-49.

Holmes, K. C. (1995). The actomyosin interaction and its control by tropomyosin. *Biophys. J.* **68**, 2s-7s.

Horowitz, J. A. and Hammer, J. A. (1990). A new *Acanthamoeba* myosin heavy chain. *J. Biol. Chem.* **265**, 20646-20652.

Hudspeth, A. J. and Gillespie, P. G. (1994). Pulling springs to tune transduction: adaptation by hair cells. *Neuron* **12**, 1-9.

Huxley, A. F. (1957). Muscle structure and theories of contraction. *Prog. Biophys. Chem.* **7**, 225-318.

Huxley, H. E. (1969). The mechanism of muscular contraction. *Science* **164**, 1356-1366.

Huxley, A. F. and Simmons, R. M. (1971). Proposed mechanism of force generation in striated muscle. *Nature* **233**, 533-538.

Huxley, A. F. (1974). Muscular contraction. *J. Gen. Physiol.* **243**, 1-43.

Ishijima, A., Harada, Y., Kojima, H., Funatsu, T., Higuchi, H. and Yanagida, T. (1994). Single-molecule analysis of the actomyosin motor using nano-manipulation. *Biochem. Biophys. Res. Commun.* **199**, 1057-1063.

Itakura, S., Yamakawa, H., Toyoshima, Y. Y., Ishijima, A., Kojima, T., Harada, Y., Yanagida, T., Wakabayashi, T. and Sutoh, K. (1993). Force-generating domain of myosin motor. *Biochem. Biophys. Res. Commun.* **196**, 1504-1510.

Johnston, G.C., Prendergast, J.A. and Singer, R.A. (1991). The *Saccharomyces cerevisiae* MYO2 gene encodes an essential myosin for vectorial transport of vesicles. *J. Cell Biol.* **113**, 539-551.

Kabsch, W., Mannherz, H. G., Suck, D., Pai, E. F. and Holmes, K. C. (1990). Atomic structure of the actin-DNase complex. *Nature* **347**, 37-44.

Kellerman, K. A. and Miller, K. G. (1992). An unconventional myosin heavy chain gene from *Drosophila melanogaster*. *J. Cell Biol.* **119**, 823-834.

Kiehart, D. P. (1990). Molecular genetic dissection of myosin heavy chain function. *Cell* **60**, 347-350.

Kinkema, M. and Schiefelbein, J. (1994). A myosin from a higher plant has structural similarities to class V myosins. *J. Mol. Biol.* **239**, 591-597.

Kinkema, M., Wang, H. and Schiefelbein, J. (1994). Molecular analysis of the myosin gene family in *Arabidopsis thaliana*. *Plant. Mol. Biol.* **26**, 2239-2253.

Kishino, A. and Yanagida, T. (1988). Force measurements by micromanipulation of a single actin filament by glass needles. *Nature* **334**, 74-76.

Knight, A. E. and Kendrick-Jones, J. (1993). A myosin-like protein from a higher plant. *J. Mol. Biol.* **231**, 148-154.

Korn, E. D. and Hammer, J. A. (1988). Myosins of non-muscle cells. *Annu. Rev. Biophys. Chem.* **17**, 23-45.

Korn, E. D. and Hammer, J. A. (1990). Myosin I. *Current Opinion in Cell Biol.* **2**, 57-61.

Kretsinger, R. H. and Kawasaki, H. (1994). Calcium-binding proteins 1: EF-hands. *Protein Profile* Vol. 1, Issue 4.

Kron, S. J. and Spudich, J. A. (1986). Fluorescent actin filaments move on myosin fixed to a glass surface. *Proc. Natl. Acad. Sci. USA* **83**, 6272-6276.

Kuehne (1864). Protoplasma. *Lehrbuch der physiologische chemie* VII.

Kuo, S. C. and Sheetz, M. P. (1993). Force of single kinesin molecules measured with optical tweezers. *Science* **260**, 232-234.

Langford, G. M. (1995). Actin- and microtubule-dependent organelle motors: interrelationship between the two motility systems. *Curr. Opin. Cell Biol.* **7**, 82-88.

Lesk, A. and Chothia, C. (1984). Mechanisms of domain closure in proteins. *J. Mol. Biol.* **174**, 175-191.

Lillie, S. H. and Brown S. S. (1992). Suppression of a myosin defect by a kinesin related gene. *Nature* **356**, 358-361.

Lillie, S. H. and Brown S. S. (1994). Immunofluorescence localization of the

unconventional myosin, Myo2p, and the putative kinesin-related protein, Smy1p, to the same regions of polarized growth in *Saccharomyces cerevisiae*. *J. Cell Biol.* **125**, 825-842.

Lowey, S., Slayter, H. S., Weeds, A. G., Baker, H. (1969). Substructure of the myosin molecule I: Subfragments of myosin by enzymic degradation. *J. Mol. Biol.* **42**, 1-29.

Lowey, S., Waller, G. S. and Trybus, K. M. (1993). Skeletal muscle myosin light-chains are essential for physiological speeds of shortening. *Nature* **365**, 454-456.

Lymn, R. W. and Taylor E. W. (1971). Mechanism of adenosine triphosphate hydrolysis of actomyosin. *Biochem.* **10**, 4617-4624.

Maddox, J. (1994). More models of muscle movement. *Nature* **368**, 287.

Margossian, S. S. and Lowey, S. (1982). Preparation of myosin and its subfragments from rabbit skeletal muscle. In *Methods in Enzymology* vol. **85** (ed. D. W. Frederiksen and L. W. Cunningham), pp. 55-71. Academic Press: New York.

Martindale, D. W. 1989. Codon usage in *Tetrahymena* and other ciliates. *J. Protozool.* **36**, 29-34.

McLaughlin, P. J., Gooch, J. T., Mannherz, H. G. and Weeds, A. G. (1993). Structure of gelsolin segment of 1 actin complex and the mechanism of filament severing. *Nature* **364**, 685-692.

Mercer, J. A., Seperack, P. K., Stobel, M. C., Copeland, N. G. and Jenkins, N. A. (1991). Novel myosin heavy chain encoded by murine *dilute* coat color locus. *Nature* **349**, 709-713.

Mermall, V., McNally, J. G. and Miller, K. G. (1994). Transport of cytoplasmic particles catalysed by an unconventional myosin in living *Drosophila* embryos. *Nature* **369**, 560-562.

Mermall, V. and Miller, K. G. (1995). The 95F unconventional myosin is required for proper organization of the *Drosophila* syncytial blastoderm. *J. Cell Biol.* **129**, 1575-1588.

Metenier, G., (1984). Actin in *Tetrahymena paravorax* : ultrastructural localization of HMM-binding filaments in glycinerated cells. *J. Protozool.* **31**, 295-215.

Miyamoto, H., Nihonmatsu, I., Kondo, S., Ueda, R., Togashi, S., Hirata, K., Ikegami, Y. and Yamamoto, D. (1995). Canoe encodes a novel protein containing a GLGF/DHR motif and functions with Notch and scabrous in common developmental pathways in *Drosophila*. *Genes Dev.* **9**, 612-625.

Molloy, J. E., Burns, J. E., Kendrick-Jones, J., Tregear, R. T. and White, D. C. S. (1995). Movement and force produced by a single myosin head. *Nature* **378**, 209-212.

Montell, C. and Rubin, G. M. (1988). The *Drosophila* ninaC locus encodes two photoreceptor cell specific proteins with domains homologous to protein kinases and the myosin heavy chain head. *Cell* **52**, 757-772.

Mooseker, M. S., Wolenski, J. S., Coleman, T. R., Hayden, S. M., Cheney, R. E., et al. (1991). Structural and functional dissection of a membrane-bound mechanoenzyme:brush border myosin I. In *Ordering the Membrane-Cytoskeleton Trilayer. Curr. Topics in Membranes.* **38**, 31-55.

Mooseker, M. S. and Cheney, R. E. (1995). Unconventional myosins. *Annu. Rev. Cell Dev. Biol.* **11**, 633-675.

Mornet, D., Pantel, P., Audemard, E. and Kassab, R. (1979). The limited tryptic cleavage of chymotryptic S1: An approach to the characterization of the actin site in myosin heads. *Biochem. Biophys. Res. Commun.* **89**, 925-932.

Nobes, C. D. and Hall, A. (1995). Rho, Rac, and Cdc42 GTPases regulate the assembly of multimolecular focal complexes associated with actin stress fibers, lamellipodia, and filopodia. *Cell* **81**, 53-62.

Ochman, H., Gerber, A. S. and Hartl, D. L. (1988). Genetic applications of an inverse polymerase chain reaction. *Genetics* **120**, 621-625.

Pate, E., White, H. and Cooke, R. (1993). Determination of the myosin step size from mechanical and kinetic data. *Proc. Natl. Acad. Sci. USA* **90**, 2451-2455.

Pollard, T. D. and Korn, E. D. (1973). *Acanthamoeba* myosin: I. Isolation from *Acanthamoeba castellanii* of an enzyme similar to muscle myosin. *J. Biol. Chem.* **248**, 4682-4690.

Pollard, T. D., Doberstein, S. K. and Zot, H. G. (1991). Myosin I. *Ann. Rev. Physiol.* **53**, 653-681.

Pollard, T. D. (1982). Assays for myosin. In *Methods in Enzymology*, vol. 85. (ed. D. W. Frederiksen and L. W. Cunningham), pp. 123-131. Academic Press: New York.

Ponting, C. P. (1995). AF-6/cno: neither a kinesin nor a myosin, but a bit of both. *Trends Biochem. Sci.* **20**, 265-266.

Porter, J. A., Hicks, J. L., Williams, D. S. and Montell, C. (1992). Differential localizations of and requirements for the two *Drosophila* ninaC kinase/myosins in photoreceptor cells. *J. Cell Biol.* **116**, 683-693.

Porter, J. A. and Montell, C. (1993). Distinct roles of the *Drosophila* ninaC

kinase and myosin domains revealed by systematic mutagenesis. *J. Cell Biol.* **122**, 601-612.

Porter, J. A., Yu, M., Doberstein, S. K., Pollard, T. D. and Montell, C. (1993). Dependence of calmodulin localization in the retina on the ninaC unconventional myosin. *Science* **262**, 1038-1042.

Porter, J. A., Minke, B. and Montell, C. (1995). Calmodulin binding to *Drosophila* NinaC required for termination of phototransduction. *EMBO J.* **14**, 4450-4459.

Prasad, R., Gu. Y., Alder, H., Nakamura, T., Canaani, O., Saito, H., Huebner, K., Gale, R. P., Nowell, P. C. and Kuriyan, K. (1995). Cloning of the ALL-1 fusion partner, the AF-6 gene, involved in acute myeloid leukemias with the t(6;11) chromosome translocation. *Cancer Res.* **53**, 5624-5628.

Prescott, D. M. (1995). The DNA of ciliated protozoa. *Microbiol. Revs.* **58**, 233-267.

Rawn, J. D. (1989). Contractile proteins and the cytoskeleton. In *Biochemistry.* (Carolina Biological Supply) pp. 1077-1105.

Rayment, I., Rypniewski, W. R., Schmidt-Base, K., Smith, R., Tomchick, D. R., Benning, M. M., Winkelmann, D. A., Wesenberg, G. and Holden H. M. (1993a). Three-dimensional structure of myosin subfragment-1: a molecular motor. *Science* **261**, 50-57.

Rayment, I., Holden, H. M., Whittaker, M., Yohn, C. B., Lorenz, M., Holmes, K. C. and Milligan, R. A. (1993b). Structure of the actin-myosin complex and its implications for muscle contraction. *Science* **261**, 58-65.

Rayment, I. and Holden, H. (1994). The three dimensional structure of a molecular motor. *Trends Biol. Sci.* **19**, 129-134.

Reinach, F. C. and Farah, C. S. (1995). The troponin complex and regulation of muscle contraction. *FASEB J.* **9**, 755-767.

Reinhard, J., Scheel., A. A., Diekmann, D., Hall, A., Ruppert, C. and Bähler, M. (1995). A novel type of myosin implicated in signaling by rho family GTPases. *EMBO J.* **14**, 697-704.

Ruppel, K. M. and Spudich, J. A. (1995). Myosin motor function: Structural and mutagenic approaches. *Curr. Opin. Cell Biol* **7**, 89-93.

Rypniewski, W. R., Holden, H. M. and Rayment, I. (1993). Structural consequences of reductive methylation of lysine residues in hen egg white lysozyme: an X-ray analysis at 1.8 A° resolution. *Biochem.* **32**, 9851-9858.

Sanders, G., Lichte, B., Meyer, H. E. and Kilimann, M. W. (1992). cDNA

encoding the chicken ortholog of the mouse *dilute* gene product. *FEBS Lett.* **311**, 295-298.

Sanger, F., Nicklen, S. and Coulson, A. (1977). DNA sequencing with chain terminating inhibitors. *Proc. Natl. Acad. Sci. USA* **74**, 5463-5467.

Schnapp, B. J. N. (1995). Molecular motors. Two heads are better than one. *Nature* **373**, 655-656.

Schroder, R. R., Manstein, D. J., Jahn, W., Holden, H., Rayment, I., Helmong, K. and Spudich, J. A. (1993). Three dimensional atomic model of F -actin decorated with *Dictyostelium* myosin S1. *Nature* **364**, 171-174.

Schutt, C. E. and Lindberg, U. (1992). Actin as the generator of tension during muscle contraction. *Proc. Natl. Acad. Sci. USA* **89**, 319-323.

Schutt, C. E., Myslick, J. C., Rozycki, M. D., Goonesekere, N. C. W. and Lindberg, U. (1993). The structure of crystalline profilin-ß-actin. *Nature* **365**, 810-816.

Schutt, C. E. and Lindberg, U. (1993). A new perspective on muscle contraction. *FEBS Lett.* **325**, 59-62.

Sellers, J. R. and Homsher, E. (1991). A giant step for myosin. *Macromolec. Struct.* **1**, 347-349.

Sheetz, M. P. and Spudich, J. A. (1983). Movement of myosin-coated fluorescent beads on actin cables *in vitro*. *Nature* **303**, 31-35.

Sheterline, P. and Sparrow, J. C. (1994). Actin. *Protein Profile* Vol. 1, Issue 1.

Shriver, J. W. (1984). Energy transduction in myosin. *Trends Biochem. Sci.* **9**, 322-328.

Shulz, G. E. (1991). Domain motions in proteins. *Curr. Opin. Struct. Biol.* **1**, 883-888.

Siemankowski, R. F. and White, H. D. (1984). Kinetics of the interaction between actin, ADP, and cardiac myosin-S1. *J. Biol. Chem.* **259**, 5045-5053.

Silvers, W. K. (1979). *Dilute* and *Leaden*, the *p*-locus, *Ruby-eye*, and *Ruby-eye-2*. In coat colors of mice: A model for mammalian gene action and interaction, ed. W. K. Silvers, New York:Springer Verlag. 83-107.

Smith, C. A. and Rayment, I. (1995). X-ray structure of the magnesium (II)-pyrophosphate complex of the truncated head of *Dictyostelium discoideum* myosin to 2.7 A resolution. *Biochem.* **34**, 8973-8981.

Solc, C. F., Derfler, R. H., Duyk, G. M. and Corey, D. R. (1994). Molecular

cloning of myosins from the bullfrog saccular macula: a candidate for the hair cell adaptation motor. *Aud. Neurosci.* **1**, 63-75.

Sowerby, A. J., Seehra, C. K., Lee, M. and Bagshaw, C. R. (1993). Turnover of fluorescent nucleoside triphosphates by isolated immobilized myosin filaments. *J. Mol. Biol.* **234**, 114-123.

Spudich, J. A. (1989). In pursuit of myosin function. *Cell Reg.* **1**, 1-11.

Spudich, J. A. (1994). How molecular motors work. *Nature* **372**, 515-518.

Steel, K. P. and Brown, S. D. M. (1994). Genes and deafness. *Trends Gen.* **10**, 428-435.

Svoboda, K. and Block, S. M. (1994). Force and velocity measured for single kinesin molecules. *Cell* **77**, 773-784.

Sweeney, H. L., Straceski, A., Leinwand, L., Tikunov, B. and Faust, L. (1994). Heterologous expression and characterization of a cardiac myosin mutant that causes hypertrophic cardiomyopathy. *J. Biol. Chem.* **269**, 1603-1605.

Taylor, E. W. (1991). Kinetic studies on the association and dissociation of myosin subfragment-1 and actin. *J. Biol. Chem.* **266**, 294-302.

Tan, J. L., Ravid, S., and Spudich, J. A. (1992). Control of nonmuscle myosins by phosphorylation. *Annu. Rev. Biochem.* **61**, 721-759.

Titus, M. A. (1993). Myosins. *Curr. Opin. Cell Bioll.* **5**, 77-81.

Titus, M. A., Kuspa, A. and Lumis, W. F. (1994). Discovery of myosin genes by physical mapping in *Dictyostelium. Proc. Natl. Acad. Sci. USA.* **91**, 9446-9450.

Toyoshima, Y. Y., Kron, S.J., McNally, E. M., Niebling, K. R., Toyoshima, C. and Spudich, J. A. (1987). Myosin subfragment-1 is sufficient to move actin filaments in vitro. *Nature* **328**, 536-539.

Triglia, T., Peterson, M. G. and Kemp, D. J. (1988). A procedure for *in vitro* amplification of DNA segments that lie outside the boundaries of known sequences. *Nucleic Acids Res.* **16**, 8186.

Uyeda, T. Q. P. and Spudich, J. A. (1993). A functional recombinant myosin II lacking a regulatory light chain binding site. *Science* **262**, 1867-1870.

Uyeda, T. Q. P., Ruppel, K. M. and Spudich, J. A. (1994). Enzymatic activities correlate with chimaeric substitutions at the actin-binding face of myosin. *Nature* **368**, 567-569.

Vale, R. D. (1994). Getting a grip on myosin. *Cell* **78**, 733-737.

Warrick, H. M. and Spudich, J. A. (1987). Myosin structure and function in cell motility. *Annu. Rev. Cell Biol.* **3**, 379-421.

Weil, D., Blanchard, S., Kaplan, J., Guilford, P., Gibson, F., Walsh, J., Mburu, P., Valera, A., Levilliers, J., Weston, M. D. et al. (1995). Defective myosin VIIA gene responsible for Usher syndrome type 1B. *Nature* **374**, 60-61.

White, H. D. and Rayment, I. (1993). Kinetic characterization of reductively methylated myosin subfragment-1. *Biochem.* **32**, 9859-9865.

Wolenski, J. S. (1995). Regulation of calmodulin binding myosins. *Trends Cell Biol.* **5**, 310-316.

Xie, X., Harrison, D. H., Schlichting, I., Sweet, R. M., Kalabokis, V. N., Szent-Gyorgyi, A. G. and Cohen, C. (1994). Structure of the regulatory domain of scallop myosin at 2.8 Aº resolution. *Nature* **368**, 306-312.

Yanagida, T. and Ishijima, A. (1995). Forces and steps generated by single myosin molecules. *Biophys. J.* **68**, 312s-320s.

Yin, H., Wang, M. D., Svoboda, K., Landick, R., Block, S. and Gelles, J. (1995). Transcription against an applied force. *Science* **270**, 1653-1657.

Yount, R. G., Lawson, D. and Rayment, I. (1995). Is myosin a "back-door" enzyme? *Biophys. J.* **68**, 44s-47s.